*Advanced Materials Research* *Online: 2016-08-22*
*ISSN: 1662-8985, Vol. 1141, pp 156-161*
*doi:10.4028/www.scientific.net/AMR.1141.156*


# Heating Rate and Composition Dependence of Crystallization Temperature of Cu-Based Metallic Glasses

Supriya Kasyap, Sonal Prajapati and Arun Pratap[a]

Condensed Matter Physics Laboratory, Applied Physics Department, Faculty of Technology and Engineering, The M. S. University of Baroda, Vadodara -390001, India

[a]apratapmsu@yahoo.com

**Keywords:** Onset Crystallization Temperature ($T_x$), Peak Crystallization Temperature ($T_p$), metallic glasses

**Abstract.** The variation of onset of crystallization temperature ($T_x$) and peak crystallization temperature ($T_p$) with heating rate ($q$) is studied. $T_x$ and $T_p$ vary in a power law behavior with heating rate ($q$) for $Cu_{60}$ $Zr_{20}Ti_{20}$ metallic glass and these parameters show a linear variation for $Cu_{60}Zr_{40}$ metallic glass. The power law variation is expressed as $T_x$ (or $T_p$) = $T_0$ $[q]^y$; where, $q$ is the normalized heating rate, $T_0$ is the $T_x$ (or $T_p$) at a heating rate of $1^0 Cmin^{-1}$. Further, the calculated values of $T_x$ (or $T_p$) are found to be in good agreement with the experimental results. Hence, the power law relation is found to be an appropriate theoretical expression for the variation of crystallization temperature ($T_x$ or $T_p$) with heating rate ($q$) for $Cu_{60}$ $Zr_{20}Ti_{20}$ metallic glass. In addition to heating rate, the composition of a metallic glass also affects its crystallization temperature. It is observed that the characteristics temperatures shift towards higher values with increase in number of components.

## Introduction

Metallic glasses are one of the best structural and functional materials now days due to their excellent properties such as corrosion and wear resistance, high strength, etc. These properties depend on the structure of metallic glasses, which is meta-stable in nature. The study of its structure becomes more important from the application point of view. To understand the stability of disordered structure, thermal treatment can be employed. Inoue et al [1] and Kovneristyj et al [2] have reported excellent thermal and mechanical properties of Cu-Zr-Ti alloys. $Cu_{60}Ti_{20}Zr_{20}$ metallic glass is found to have highest glass forming ability (GFA) among various compositions of Cu-Zr-Ti alloys [1]. Due to its high glass forming ability, various studies have been carried out on this metallic glass for understanding its crystallization kinetics [3-5]. Metallic glasses if subjected to thermal treatment exhibits some characteristics temperatures i.e., the glass transition temperature ($T_g$), the onset of crystallization temperature ($T_x$), melting temperature ($T_m$), etc. These temperatures mark the initiation of various phase changes occurring in the amorphous alloy, such as $T_g$, $T_x$, and $T_m$ indicates beginning of glass transition, crystallization, and melting processes. Furthermore, these temperatures show a variation with heating rates employed. Many approximations are available in literature to study temperature variation with heating rate [6-13]. Most of the methods suggest that $T_x$ depends linearly on heating rate, but this may not be true for all the cases.

In present study, the variation of $T_x$ and $T_p$ with heating rate is studied for Cu-based metallic glasses. It is found that both onset crystallization temperature and peak crystallization temperature show an increasing trend with heating rates employed. It shows the kinetic nature of these transition temperatures. It follows a power law equation [6] for $Cu_{60}Zr_{20}Ti_{20}$ metallic glass and a linear variation for binary amorphous alloy $Cu_{60}Zr_{40}$. The information about $T_x$ and $T_p$ at different heating rates helps in finding the activation energy of crystallization for metallic glasses by the use of various iso-kinetic and iso-conversional methods. Further, it is found that substitution of Ti for Zr in $Cu_{60}Zr_{40}$ metallic glass increases the value of $T_x$ and therefore its glass forming ability.

## Experimental

The amorphous alloy of composition $Cu_{60}Zr_{20}Ti_{20}$ was prepared in ribbon form by single roller melt spinning technique at the Institute of Material Research, Tohoku University, Sendai, Japan. Argon atmosphere was used for the preparation of sample to avoid oxidation. XRD and TEM analysis were done to confirm the amorphous nature of $Cu_{60}Zr_{20}Ti_{20}$ metallic glass. The thermal analysis of $Cu_{60}Zr_{20}Ti_{20}$ metallic glass was done in DSC 2910 (TA Instruments Inc., USA) system using modulated DSC mode at four different heating rates ($q$) i.e., 1, 2, 4, and $8^0$C min$^{-1}$. The MDSC thermo-grams indicated a two step crystallization process at all the heating rates.

## Theory

The variation of crystallization temperature with heating rates can be understood in terms of power law equation [6], i.e,

$$T_x = T_0 [q]^y \tag{1}$$

Where, $q$ is the normalized heating rate, $T_0$ is the $T_x$ at a heating rate of $1^0$Cmin$^{-1}$. Normalization has been done with respect to heating rate of $1^0$C min$^{-1}$.
Using eq. (1) exponent $y$ can be calculated as

$$y = \log_{10}\left[\frac{(T_x)_\alpha}{(T_x)_1}\right]\left[\log_{10}[q]\right]^{-1} \tag{2}$$

Where $(T_x)_\alpha$ represents $T_x$ at any arbitrary heating rate and $(T_x)_1$ represents $T_x$ at $1^0$C min$^{-1}$ (i.e., $T_0$). In a similar way $T_p$ variation with $q$ can be written as

$$T_p = T_0 [q]^y \tag{3}$$

Where $y$ can be calculated as

$$y = \log_{10}\left[\frac{(T_p)_\alpha}{(T_p)_1}\right]\left[\log_{10}[q]\right]^{-1} \tag{4}$$

Here, $(T_p)_\alpha$ and $(T_p)_1$ are value of $T_p$ at any arbitrary heating rate and the same at $1^0$C min$^{-1}$ respectively.

## Results and discussion

The crystallization temperature ($T_x$) represents the onset of crystallization process and the peak crystallization temperature ($T_p$) represents the temperature of the peak of crystallization event. Both $T_x$ and $T_p$ show a significant variation with heating rate ($q$). $T_x$ and $T_p$ are shifted to higher temperatures with increasing heating rates, which implies that crystallization depends upon heating rate during continuous heating [14-15]. Activation energy corresponding to each characteristic temperature, i.e., $T_x$ and $T_g$, can be evaluated through different iso-conversional and iso-kinetic methods [3].

Figure-1 represents the variation of theoretically calculated $T_x$ values with heating rate $q$ for both the crystallization peaks along with experimental points. It can be seen that the calculated $T_x$ values vary in accordance with the experimental $T_x$ values. The variation of theoretically calculated and experimental $T_p$ values is shown in figure-2, for both crystallization peaks. Both calculated and experimental values of $T_p$ are found to be in good agreement with each other. Hence, it can be seen that the power law equation is a suitable tool for understanding the variation of crystallization temperatures with heating rate. Using this concept of variation of $T_x$ (or $T_p$) with heating rate ($q$), the activation energy for the crystallization of metallic glasses can be determined using different iso-kinetic and iso-conversional methods.

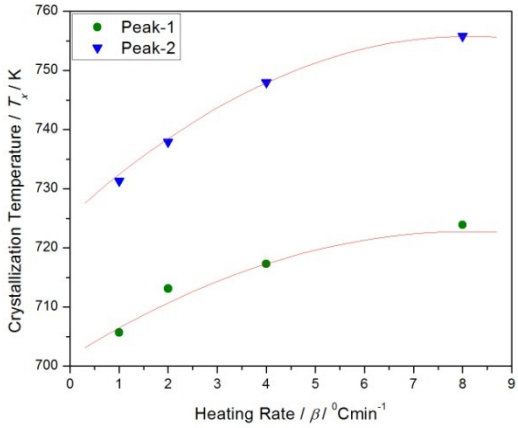


Fig.1. Variation of onset of crystallization temperature ($T_x$) with heating rate ($q$):(——) represents theoretically calculated results using Eq. 3; (●,▼) represents experimental points for peak 1 & 2 respectively for $Cu_{60}Zr_{20}Ti_{20}$ metallic glass

$T_x$ and $T_p$ are inversely proportional to the relaxation time which in turn varies inversely with heating rate ($q$). Hence $T_x$ and $T_p$ increases with increasing heating rate. At slower heating rates, the randomly arranged structure relaxes more easily and hence the metallic glass starts crystallizing at a lower temperature, and vice-versa. Among various other factors that affect the value of $T_x$ in a metallic glass, atomic size mismatch is one. It was suggested that a greater size mismatch among constituent atoms leads to a higher value of $T_x$. Reduction in free volume & diffusivity, electron to atom ratio, differences in electro-negativities, are few other factors that are responsible for variation in $T_x$.

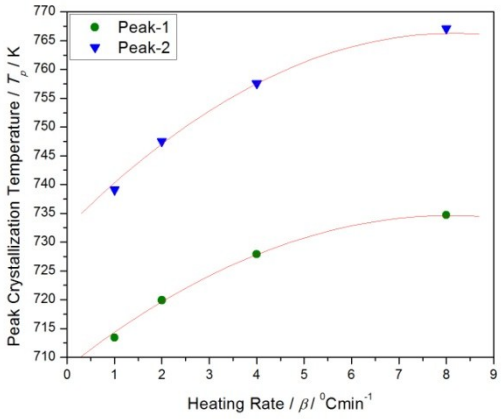


Fig.2. Variation of peak crystallization temperature ($T_p$) with heating rate ($q$): ( ——) represents theoretically calculated results using Eq. 3; (●,▼ ) represents experimental points for peak 1 & 2 respectively for $Cu_{60}Zr_{20}Ti_{20}$ metallic glass

Table 1 Experimental $T_x$ and $T_p$ values at different heating rates for $Cu_{60}Zr_{40}$ and $Cu_{60}Zr_{20}Ti_{20}$ metallic glasses for peak 1

| **$Cu_{60}Zr_{40}$ [16]** | | | **$Cu_{60}Zr_{20}Ti_{20}$** | | |
|---|---|---|---|---|---|
| **Heating rate ($^0$Cmin-1)** | **$T_x$ (K)** | **$T_p$ (K)** | **Heating rate ($^0$Cmin-1)** | **$T_x$ (K)** | **$T_p$ (K)** |
| 5 | 705 | 715 | 1 | 705 | 713 |
| 10 | 707 | 723 | 2 | 713 | 719 |
| 15 | 709 | 726 | 4 | 717 | 727 |
| 20 | 711 | 729 | 8 | 723 | 734 |

Table 1 represents experimental $T_x$ and $T_p$ values at different heating rates for $Cu_{60}Zr_{40}$ and $Cu_{60}Zr_{20}Ti_{20}$ metallic glasses. It can be observed that the characteristics temperatures shift towards higher values with increase in heating rates and number of components. A higher value of $T_x$ represents greater GFA of metallic glass. In present case $T_x$ value at $q=5^0Cmin^{-1}$ for binary system is equivalent to the value of $T_x$ at $q=1^0min^{-1}$ for ternary system. Hence the substitution of Ti to the binary metallic glass shifts the value of $T_x$ to a higher temperature. It implies that a ternary alloy is a better glass former as compared to its respective binary counterpart. Hence, the addition of Ti to Cu-Zr binary alloy enhances its GFA significantly. Fig. 3 shows a linear variation of $T_x$ and $T_p$ with heating rate for $Cu_{60}Zr_{40}$ metallic glass, given by the expression:

$$T_x \text{ (or } T_p) = A + Bq \quad (5)$$

With A and B as the slope and intercept of the plot and $q$ is the heating rate employed.

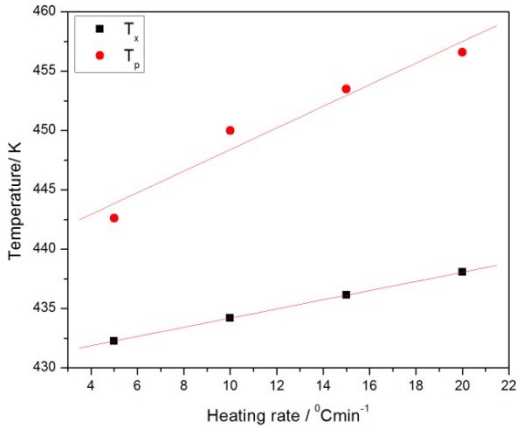


Fig.3. Variation of $T_x$ and $T_p$ with heating rate for $Cu_{60}Zr_{40}$ metallic glass [16]

The three empirical rules given by Inoue et al [17] for glass formation are: (i) large number of components, (ii) size mis-match between the various components, and (iii) negative heat of mixing. More number of components is supposed to increase the GFA of metallic glasses by making the structure of glassy alloy denser and randomly packed with a short range order. Hence, ternary alloy $Cu_{60}Zr_{20}Ti_{20}$ is a better glass former than $Cu_{60}$ $Zr_{40}$. Secondly, a greater size difference (>12%) between different components increases the GFA of metallic glasses. The addition of elements of different radii increases the entropy of disorder and hence makes it difficult for the components to acquire their stable configuration. Here, the atomic radius of Cu, Zr and Ti are 0.128 nm, 0.160 nm and 0.147 nm respectively. This size difference is sufficient to make the interchangeability between the different components difficult. Large size difference destabilizes the crystalline phase by increasing the internal energy of the crystalline solid solution. The prime root of metallic glass formation lies in destabilizing the competing crystalline phases. This destabilization of crystalline phases can be achieved by atomic pair formation between unlike components with large size difference [18-20]. Formation of local crystalline structure, in alloys with same atomic sized components, is shown by Yun et al [20]. Hence, a greater GFA is crucially favored by a large size mis-match and a large negative heat of mixing. The substitution of Zr by Ti makes the interchangeability among the components of the alloy easy, since Ti and Zr belong to the same group in periodic table and share common characteristics. Hence Ti becomes a suitable candidate for changing composition of metallic glass from $Cu_{60}Zr_{40}$ to $Cu_{60}Zr_{20}Ti_{20}$. Thirdly, negative heat of mixing favors glass formation by coercing the formation of atomic pair between different components, which in turn increases the difficulty of atomic rearrangement in a glassy alloy during heating. The heats of mixing for atomic pairs Cu-Zr, Zr-Ti and Ti-Cu are -23, 0 and -9 kJ $mol^{-1}$ respectively [21]. These interactions are much weaker as compared to those atomic interactions in quaternary and quinary alloys such as $Zr_{55}Cu_{30}Al_{10}Ni_5$ and $Zr_{41}Ti_{14}Cu_{12.5}Ni_{10}Be_{22.5}$. The heats of mixing for atomic pairs in $Zr_{55}Cu_{30}Al_{10}Ni_5$ and $Zr_{41}Ti_{14}Cu_{12.5}Ni_{10}Be_{22.5}$ alloys are 0, -23, -49, -43, -44, -22, -9, -35 and -30 $kJmol^{-1}$ respectively for Zr-Ti, Zr-Cu, Zr-Ni, Zr-Be, Zr-Al, Al-Ni, Ti-Cu, Ti-Ni and Ti-Be [21]. These atomic interactions can also be understood in terms of

pre-exponential factor ($k_0$). $k_0$ provides information about the number of jumps nuclei make per unit time in order to overcome the activation energy barrier. In general, it gives information about atomic mobility. $k_0$ can be obtained by least square fitting of the crystallized fraction versus temperature curve. In our previous work [3], we have done the Iterative least-square fitting to the experimental data of fractional crystallization for $Cu_{60}Zr_{20}Ti_{20}$ metallic glass, and obtained the values of $k_0$ to be of the order $10^{22}$and $10^{17}$ $s^{-1}$ for first and second peak respectively. Typical Zr based BMGs exhibit $k_0$ of the order of $10^{12}$ $s^{-1}$ for first crystallization peak, such as the value of $k_0$ for $Zr_{55}Cu_{30}Al_{10}Ni_5$ and $Zr_{41}Ti_{14}Cu_{12.5}Ni_{10}Be_{22.5}$ BMGs are 4.2 $x10^{12}s^{-1}$ and 1.0 x $10^{12}s^{-1}$ respectively [22-23]. This indicates that the value of $k_0$ for $Cu_{60}Zr_{20}Ti_{20}$ metallic glass is much higher than that of Zr-based quaternary and quinary BMGs. This may be due to the reason that quaternary and quinary BMGs are supposed to have higher degree of dense random packing as compared to that of the ternary alloy. Further $k_0$ is greatly influenced by the configuration and atomic interactions between the various components of the alloy. The atoms of an alloy, with high degree of dense random packing, require greater energy to overcome the interatomic interactions. The mobility of atoms in alloys with strong interatomic interactions is less than the alloys with weak interatomic interactions. The heats of mixing of atomic pairs in quaternary and quinary BMGs are higher than that of the ternary alloy. Hence $Zr_{55}Cu_{30}Al_{10}Ni_5$ and $Zr_{41}Ti_{14}Cu_{12.5}Ni_{10}Be_{22.5}$ BMGs exhibit relatively smaller values of $k_0$ as compared to $Cu_{60}$ $Zr_{20}Ti_{20}$ metallic glass.

## Conclusion

In order to study the stability of metallic glasses, it is required to understand their behavior towards crystallization event. Crystallization is characterized by the onset of crystallization temperature ($T_x$) and peak crystallization temperature ($T_p$). This study provides an insight of heating rate and composition dependence of crystallization temperature. Both the crystallization temperature ($T_x$) and the peak crystallization temperature ($T_p$) are found to follow a power law variation with heating rate for $Cu_{60}$ $Zr_{20}Ti_{20}$ metallic glass. It also provides information about the heating rate suitable for crystallization of a melts. In absence of sufficient experimental data one can make use of theoretical formulae for deriving useful conclusions regarding the kinetics of crystallization. $Cu_{60}$ $Zr_{40}$ binary alloy follows a linear variation for both the characteristic temperatures i.e., $T_x$ and $T_p$ respectively. Further, an addition of Ti to binary alloy increases the characteristic temperatures, which enhances the GFA. Hence, an increase in number of components increases the GFA of a metallic glass.

## Acknowledgements

One of the authors (Supriya Kasyap) is grateful to the University Grant Commission (UGC), New Delhi for providing the financial support under Research Fellowship in Science for Meritorious Students (RFSMS) scheme. The author Sonal Prajapati is grateful to Department of Science & Technology (DST), Govt. of India, for providing financial assistance under the DST-INSPIRE fellowship scheme.

## References

[1] A. Inoue, W. Zhang, T. Zhang, K. Kurosaka, Thermal and mechanical properties of Cu-based Cu-Zr-Ti bulk glassy alloys, Mater. Trans. JIM. 42 (2001) 1149-1151.

[2] Y. K. Kovneristyj, A. G. Pashkovskaya, Bulk amorphization of alloys in the intermetallide containing system Ti–Cu–Zr, Amorf. (Stekloobraz) Met. Mater. RAN Int. Metallurgii. M. 1992; p153-157

[3] S. Kasyap, A. T. Patel, A. Pratap, Crystallization kinetics of $Ti_{20}Zr_{20}Cu_{60}$ metallic glass by iso-conversional methods using modulated differential scanning calorimetry, J. Therm. Anal. Calorim. 116 (2014) 1325-1336.

[4] A. Pratap, K. N. Lad, R. T. Savaliya, G. K. Dey, S. Banerjee, A. M. Awasthi, Kinetics of crystallization $Zr_{20}Ti_{20}Cu_{60}$ amorphous alloy using modulated differential scanning calorimetry, Phys. Chem. Glasses. 45 (2004) 258-262.

[5] A. Pratap, K. G. Raval, A. Gupta, MDSC studies of the crystallization kinetics of $Cu_{60}Zr_{20}Ti_{20}$ glass, Proc. 11th Nat. Symp. on Therm. Anal. 1998; pp.22-24.

[6] S. R. Joshi, A. Pratap, N. S. Saxena, M. P. Saksena, A. Kumar, Heating rate and composition dependence of the glass transition temperature of a ternary chalcogenide glass, J. Mater. Sci Lett. 13 (1994) 77-79.

[7] M. Lasocka, The effect of scanning rate on glass transition temperature of splat-cooled $Te_{85}Ge_{15}$. Mater. Sci. Eng. A. 23 (1976) 173-177.

[8] H. E. Kissinger, Reaction kinetics in differential thermal analysis, Anal. Chem. 29 (1957) 1702-1706.

[9] T. Akahira, T. Sunose, Joint convention of four electrical institutes, Res. Report. Chiba. Inst. Technol. (Sci. & Technol.) 16 (1971) 22-31.

[10] A. Augis, J. E. Bennett, Calculation of Avarami parameters for heterogeneous solid state reactions using modification of the Kissinger method, J. Therm. Anal. Calorim. 13 (1978) 283-292.

[11] P. G. Boswell, On the calculation of activation energies using modified Kissinger method, J. Therm. Anal. Calorim. 18 (1980) 353-358.

[12] T. Ozawa, A new method for analyzing thermogravimetric data, Bull. Chem. Soc. Jpn. 38 (1965) 1881-1886.

[13] J. H. Flynn, L. A. Wall, General treatment of the thermogravimetry of polymers, J. Res. Natl. Bur. Stand. A Phys Chem. 70A (1996) 487-523.

[14] L. Liu, Z. F. Wu, J. Zhang, Crystallization kinetics of $Zr_{55}Cu_{30}Al_{10}Ni_5$ bulk amorphous alloys, J. Alloys Compd. 339 (2002) 90-95.

[15] X. Ou, G. Q. Zhang, X. Xu, L. N. Wang, J. H. Liu, J. Z. Jiang, Crystallization kinetics in $Cu_{35}Ag_{15}Zr_{45}Al_{15}$ metallic glass, J. Alloys Compds. 441 (2007) 181-184.

[16] G. D. Ladiwala, N. S. Saxena, S. R. Joshi, A. Pratap, M. P. Saksena, Crystallization kinetics and specific heat of $Cu_{60}Zr_{40}$ glassy alloys, Mater. Sci. Engg. A. A181/A182 (1994) 1427-1430.

[17] A. Inoue, A. Takeuchi, T. Zhang, Ferromagnetic bulk amorphous alloys, Metall. Mater. Trans. A. 29 (1998) 1779-1793.

[18] O. N. Senkov, D. B. Miracle, Effect of the atomic size distribution on glass forming ability of amorphous metallic alloys, Mater. Res. Bull. 36 (2001) 2183-2198.

[19] Z. P. Lu, C. T. Liu, Y. D. Dong, Effects of atomic bonding nature and size mismatch on thermal stability and glass-forming ability of bulk metallic glasses, J. Non-Crys.t Solids. 341 (2004) 93-100.

[20] Y. S. Yun, H. S. Nam, P. R. Cha, W. T. Kim, D. H. Kim, Effects of atomic size difference and heat of mixing parameters on local structure of a model metallic glass system, Met. Mater. Int. 20 (2014) 105-111.

[21] A. Takeuchi, A. Inoue, Calculations of mixing enthalpy and mismatch entropy for ternary amorphous alloys, Mater. Trans. JIM. 41 (2000) 1372-1378.

[22] L. Liu, Z. F. Wu, J. Zhang, Crystallization kinetics of $Zr_{55}Cu_{30}Al_{10}Ni_5$ bulk amorphous alloy, J. Alloy Compd. 339 (2002) 90-95.

[23] Y. X. Zhuang, W. H. Wang, Y. Zhang, M. X. Pan, D. Q. Zhao, Crystallization kinetics and glass transition of $Zr_{41}Ti_{14}Cu_{12.5}Ni_{10-x}Fe_xBe_{22.5}$ bulk metallic glasses, Appl. Phys. Lett. 75 (1999) 2392-2394.

# *Crystallization kinetics of $Ti_{20}Zr_{20}Cu_{60}$ metallic glass by isoconversional methods using modulated differential scanning calorimetry*

**Supriya Kasyap, Ashmi T. Patel & Arun Pratap**

**Journal of Thermal Analysis and Calorimetry**
An International Forum for Thermal Studies

ISSN 1388-6150
Volume 116
Number 3

J Therm Anal Calorim (2014)
116:1325-1336
DOI 10.1007/s10973-014-3753-z

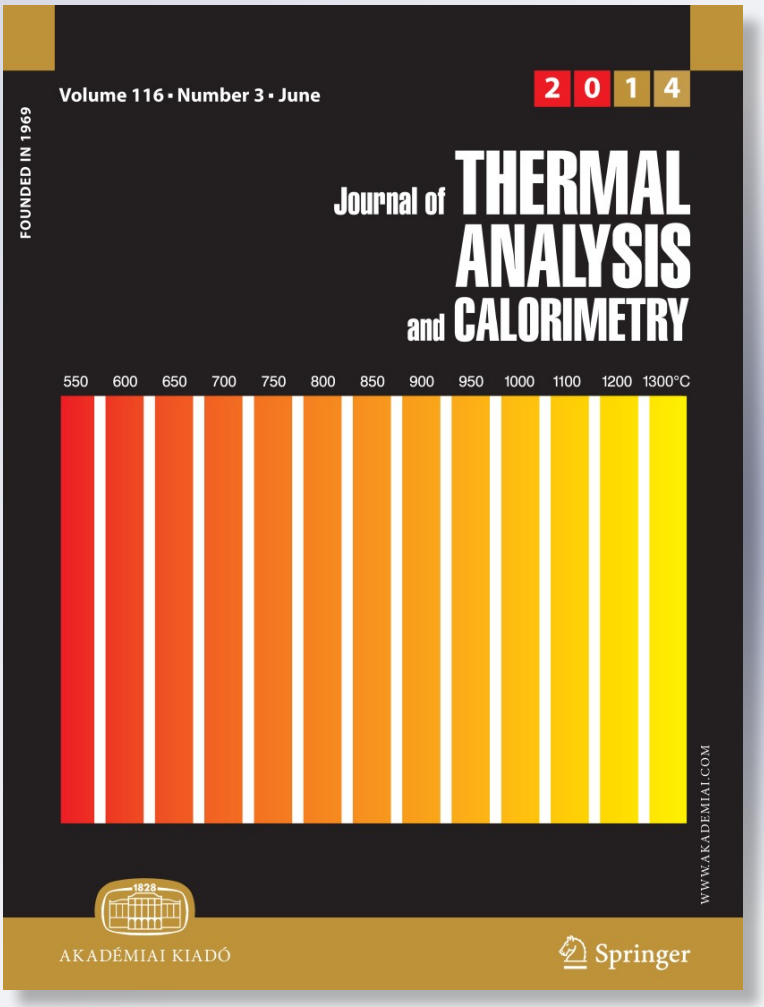


Springer

J Therm Anal Calorim (2014) 116:1325–1336
DOI 10.1007/s10973-014-3753-z

# Crystallization kinetics of $Ti_{20}Zr_{20}Cu_{60}$ metallic glass by isoconversional methods using modulated differential scanning calorimetry

**Supriya Kasyap · Ashmi T. Patel · Arun Pratap**

Received: 12 September 2013 / Accepted: 12 March 2014 / Published online: 16 April 2014


**Abstract** The study of crystallization kinetics of amorphous alloys has been a matter of great interest for material researchers for past few decades, since it provides information about the kinetic parameters i.e., activation energy of crystallization and the frequency factor. These kinetic parameters can be calculated by model-free isoconversional methods. Isoconversional methods allow calculating the activation energy as a function of degree of conversion, $\alpha$. Hence, these methods provide accurate results for multistep processes like crystallization. Model-free methods are categorized as linear and non-linear isoconversional methods. Linear methods are further classified as linear differential and linear integral isoconversional methods. In present work, we have used these isoconversional methods to study the effect of non-linear heating rate, employed by modulated differential scanning calorimetry (MDSC), on the non-isothermal crystallization kinetics of $Ti_{20}Zr_{20}Cu_{60}$ metallic glass. For $Ti_{20}Zr_{20}Cu_{60}$, MDSC curves clearly indicate a two-step crystallization process. Both crystallization peaks were studied based on the modified expressions for isoconversional methods by non-linear heating rate. The term corresponding to non-linearity comes out to be $(A_T\omega/2\beta)^2$. The effect of non-linear heating rate on measurement of kinetic parameters by isoconversional methods is studied. The activation energy of crystallization is calculated for $Ti_{20}Zr_{20}Cu_{60}$ metallic glass for various degrees of conversion by linear integral isoconversional methods i.e., Ozawa–Flynn–Wall, Kissinger–Akahira–Sunose, and also with Friedman method which is a linear differential isoconversional method.

**Keywords** Crystallization kinetics · Model-free or isoconversional methods · Differential scanning calorimetry (DSC) · Modulated differential scanning calorimetry (MDSC) · Activation energy

S. Kasyap (✉) · A. T. Patel · A. Pratap
Condensed Matter Physics Laboratory, Applied Physics Department, Faculty of Technology and Engineering, The M. S. University of Baroda, Vadodara 390001, Gujarat, India
e-mail: supriya_kasyap@yahoo.com

A. Pratap
e-mail: apratapmsu@yahoo.com

A. T. Patel
Physics Department, Institute of Technology and Management Universe, Dhanora Tank Road, Paldi Village, Waghodia Taluka, Vadodara 391510, India

## Introduction

The non-equilibrium or metastable character of metallic glasses makes them a suitable candidate for the study of their reaction toward thermal treatment. As these metastable materials are subjected to heat, the disordered structure moves toward equilibrium through primary nucleation followed by three-dimensional growth. This thermally activated process is termed as crystallization and includes diffusion of particles toward the growth front. The crystallization process can proceed through isothermal and non-isothermal routes [1–5]. The excellent thermal and mechanical properties of Cu–Zr–Ti alloys have been reported in literature [6–7]. Among various compositions of Cu–Zr–Ti alloys, $Ti_{20}Zr_{20}Cu_{60}$ is found to have the highest glass forming ability [6]. Hence, in present case, we have studied non-isothermal crystallization of $Ti_{20}Zr_{20}Cu_{60}$ metallic glass.

Crystallization kinetics involves not only the study of the rate at which a randomly arranged structure transforms into an orderly structure, but also the route of their transformation. The study of crystallization kinetics provides

the way through which a glassy structure has crystallized, thereby giving a direction to improve its properties.

Crystallization kinetics can be studied through isokinetic and isoconversional methods. Isokinetic methods assume the transformation mechanism to be same throughout the temperature or time range and allow calculating single values of the kinetic parameters such as activation energy. An isoconversional method, on the other hand, assumes the transformation mechanism at a constant degree of conversion as a function of temperature and provides kinetic parameters varying with the degree of conversion, $\alpha$. Since multi-component metallic glasses generally crystallize through multisteps, their transformation mechanism cannot be considered same throughout. It involves different mechanisms for each step and for a particular range of temperatures. Thus, one has to switch to the isoconversional methods for understanding the crystallization behavior of metallic glasses. Many studies, on crystallization kinetics by various isokinetic and isoconversional methods, are present in literature [8–11]. Recently, Lu and Li [12] have studied the kinetics of non-isothermal crystallization in Cu-based metallic glasses by using various isokinetic and isoconversional methods. Others, such as Wu et al. [13] and Svoboda and Malek [14], have used only isoconversional methods for the study of crystallization kinetics.

One of the most popular thermo-analytical techniques to study the crystallization process and its kinetics in amorphous materials is differential scanning calorimetry, DSC [15]. However, a more improvised version of DSC, known as modulated DSC (MDSC), which overcomes most of its disadvantages, is utilized scarcely for studying the crystallization kinetics. In the present study, we have made an attempt to study the kinetics of crystallization of $Ti_{20}Zr_{20}Cu_{60}$ metallic glass by isoconversional methods using MDSC.

## Experimental

Single-roller melt-spinning technique was employed to prepare amorphous ribbons of $Ti_{20}Zr_{20}Cu_{60}$ metallic glass at the Institute of Material Research, Tohoku University, Sendai, Japan. Argon atmosphere was used for the preparation of sample. XRD and TEM analyses were done to confirm the amorphous nature of $Ti_{20}Zr_{20}Cu_{60}$ metallic glass. Thermal analysis was done in DSC 2910 (TA Instruments, Inc., USA) system in MDSC mode at four different heating rates 1, 2, 4, and 8 °C $min^{-1}$.

## Theoretical background

Homogeneous reactions [16], in practice, are hard to achieve. It is vital to understand the kinetics of heterogeneous processes in order to establish product conversion rates and also for identification of the involved mechanism of the reaction. The reactions, in general, from kinetics viewpoint are classified into two types, namely isokinetic and isoconversional reactions.

### Isokinetic methods

Most of the isokinetic methods are based on the KJMA rate equation [17–21] given by

$$\frac{d\alpha}{dt} = nk(1-\alpha)[-\ln(1-\alpha)]^{(n-1)/n}, \tag{1}$$

where $\alpha$ is degree of conversion at a particular time $t$, $n$ is Avrami (growth) exponent, and $k$ is the rate constant given by

$$k(T) = k_0 \exp\left(-\frac{E}{RT}\right), \tag{2}$$

where $k_0$ is pre-exponential factor, $E$ is the activation energy, and $R$ is the universal gas constant.

From Eqs. (1) and (2) transformed fraction can be expressed as

$$\alpha = 1 - \exp\left[-\frac{k_0}{\beta}\int_{T_0}^{T}\exp\left(-\frac{E}{RT}\right)dT\right]^n. \tag{3}$$

The integral in Eq. (3) does not have an exact solution and hence one has to switch to approximations. Various approximations have been used in literature to obtain an accurate solution of the integral [22–24]. On employing Gorbachev approximation [24] i.e., Eq. (4) in Eq. (3) we obtain Eq. (5):

$$\int_0^T e^{-E/RT}dT = \frac{RT^2}{E+2RT}e^{-E/RT}, \tag{4}$$

$$\alpha = 1 - \exp\left[-\left\{\frac{k_0RT^2}{\beta(E+2RT)}\exp\left(-\frac{E}{RT}\right)dT\right\}^n\right]. \tag{5}$$

The values of $E$, $n$, and $k_0$ can be determined by fitting the experimental data of $\alpha$ to Eq. (5) with the help of method of least square.

### Isoconversional methods

The reaction rate for non-isothermal crystallization kinetics can be expressed by the following kinetic equation [25]:

$$\frac{d\alpha}{dT} = \frac{1}{\beta}k(T)f(\alpha) = \frac{k_0}{\beta}\exp\left(-\frac{E}{RT}\right)f(\alpha), \tag{6}$$

where $k(T)$ is rate constant, $\beta$ is heating rate, $\alpha$ is degree of conversion, and $f(\alpha)$ is the reaction model.

Separation of variables and integration of Eq. (6) gives:

$$g(\alpha) = \int_0^{\alpha} [f(\alpha)]^{-1} = \frac{k_0}{\beta} \int_0^{T} \exp\left(-\frac{E}{RT}\right) dT. \quad (7)$$

Since the above integral equation does not have an exact analytical solution, various approximations of this integral are suggested in literature [26–30] for evaluation of activation energies dependent on the degree of conversion, α.

The general form of the linear equation expressing the linear integral isoconversional methods is [31]:

$$\ln\left(\frac{\beta}{T_{\alpha}^{k}}\right) = -A\frac{E_{\alpha}}{RT_{\alpha}} + C, \quad (8)$$

where $k$ and $A$ are parameters depending on approximations of temperature integral, $C$ is constant, and the subscript α designates the degree of conversion. For Ozawa–Flynn–Wall, OFW ($K = 0$, $A = 1.0516$); Kissinger–Akahira–Sunose, KAS ($K = 2$, $A = 1$); and so on.

*KAS method*

KAS [32, 33] used the approximation given by Coats and Redfern [34] to evaluate the integral in Eq. (7). This method is based on the expression

$$\ln\left(\frac{\beta}{T_{\alpha}^{2}}\right) = -\frac{E_{\alpha}}{RT_{\alpha}} + \ln\left(\frac{k_0 R}{E_{\alpha}}\right). \quad (9)$$

The $E_{\alpha}$ can be calculated from the slope of the plot $\ln(\beta/T_{\alpha}^2)$ versus $1{,}000/T_{\alpha}$ for constant conversion, α.

For MDSC, the measured heating rate becomes [35]

$$\gamma = \beta + A_T\omega\cos\omega t, \quad (10)$$

where $\beta$ is the linear heating rate and the second term is due to sinusoidal temperature modulation.

Here, having a positive heating profile is very important to avoid any ambiguity in the measurement of actual heat flow associated with crystallization kinetics. The above condition can be satisfied if,

$\beta \geq A_T\omega$,

or $(A_T\omega/\beta) \leq 1$.

Substituting the heating rate employed by MDSC (Eq. (10)) in place of $\beta$ in Eq. (9), Eq. (9) becomes

$$\ln\left(\frac{(\beta + A_T\omega\cos\omega t)}{T_{\alpha}^{2}}\right) = -\frac{E_{\alpha}}{RT_{\alpha}} + \ln\left(\frac{k_0 R}{E_{\alpha}}\right), \quad (11)$$

$$\ln\left(\frac{\beta}{T_{\alpha}^{2}}\left(1 + \frac{A_T\omega\cos\omega t}{\beta}\right)\right) = -\frac{E_{\alpha}}{RT_{\alpha}} + \ln\left(\frac{k_0 R}{E_{\alpha}}\right). \quad (12)$$

Using properties of ln

$$\ln\left(\frac{\beta}{T_{\alpha}^{2}}\right) + \ln\left(1 + \frac{A_T\omega\cos\omega t}{\beta}\right) = -\frac{E_{\alpha}}{RT_{\alpha}} + \ln\left(\frac{k_0 R}{E_{\alpha}}\right). \quad (13)$$

Expanding and neglecting higher-order terms, we get

$$\ln\left(\frac{\beta}{T_{\alpha}^{2}}\right) + \sum_{n=1}^{\infty} \frac{(-1)^{n+1}\left[\frac{A_T\omega\cos\omega t}{\beta}\right]^{n}}{n} = -\frac{E_{\alpha}}{RT_{\alpha}} + \ln\left(\frac{k_0 R}{E_{\alpha}}\right), \quad (14)$$

$$\ln\left(\frac{\beta}{T_{\alpha}^{2}}\right) + \left[\left(\frac{A_T\omega\cos\omega t}{\beta}\right) - \frac{1}{2}\left(\frac{A_T\omega\cos\omega t}{\beta}\right)^{2} + \cdots\right] = -\frac{E_{\alpha}}{RT_{\alpha}} + \ln\left(\frac{k_0 R}{E_{\alpha}}\right). \quad (15)$$

Taking average over one complete cycle, Eq. (15) transforms to

$$\ln\left(\frac{\beta}{T_{\alpha}^{2}}\right) - \left(\frac{A_T\omega}{2\beta}\right)^{2} + \cdots = -\frac{E_{\alpha}}{RT_{\alpha}} + \ln\left(\frac{k_0 R}{E_{\alpha}}\right). \quad (16)$$

Equation (16) is the KAS equation using non-linear heating rate of MDSC.

Similar treatment has been done to the linear integral isoconversional methods i.e., Kissinger method, Augis and Bennett's method, Boswell method, OFW; and linear differential isoconversional methods i.e., Friedman, and Gao and Wang. The factor $(A_T\omega/2\beta)^2$ on LHS of Eq. (16) is supposed to cause non-linearity.

## Results and discussion

The MDSC experiments clearly indicate two-step crystallization process. The crystallized fraction, α, was calculated from MDSC curves and variation of α with temperature, at all the studied heating rates, and is shown in Fig. 1a, b for the two crystallization peaks, respectively. Iterative least square fitting method was used to fit the experimental data of fractional crystallization to Eq. (5). Kissinger equation was used to obtain the initial estimates of $E$ and $k_0$. The sigmoidal variation of crystallized fraction (α), with temperature indicates that crystallization occurs in bulk. Table 1 reports the values of $E$, $k_0$, and $n$ obtained by least square fitting method.

The validity of KJMA model in non-isothermal conditions can be checked by various methods available in literature [36–38]. Malek [37] proposed a simple method for checking the applicability of KJMA model. According to Malek the KJMA model is valid for studying the non-isothermal crystallization kinetics if the maximum of the function $z(\alpha)$ comes in the range (0.61–0.65). In the present study we have calculated both $y(\alpha)$ and $z(\alpha)$ as expressed in Eqs. (17) and (18), respectively:

$$y(\alpha) = \phi\exp(E/RT), \quad (17)$$

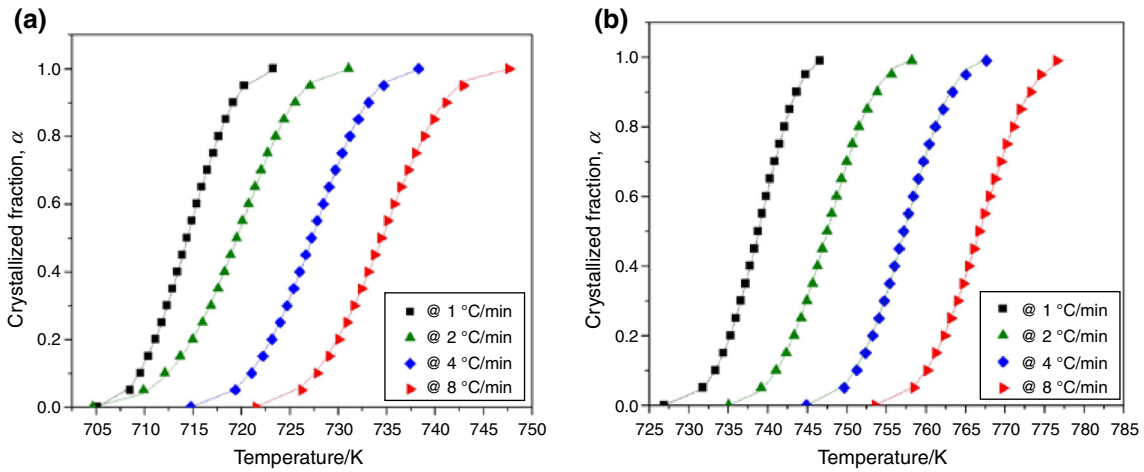


**Fig. 1** Crystallized fraction as a function of temperature for $Ti_{20}Zr_{20}Cu_{60}$ metallic glass at different heating rates; (**a**) Peak 1, (**b**) Peak 2: *symbols* represent experimental points and *solid lines* show the least square fitted curve using Eq. (5)

**Table 1** Values of Avrami (growth) exponent ($n$), pre-exponential factor ($A$), and activation energy ($E$) obtained by least square fitting of fractional crystallization data for both the crystallization peaks

| Heating rates/ °C $min^{-1}$ | KJMA (Eq. (5)) | | | | | |
|---|---|---|---|---|---|---|
| | Peak 1 | | | Peak 2 | | |
| | $n$ | $k_0/10^{22}$ $s^{-1}$ | $E$/ kJ $mol^{-1}$ | $n$ | $k_0/10^{17}$ $s^{-1}$ | $E$/ kJ $mol^{-1}$ |
| 1 | 1.91 | 1.12 | 338 | 2.34 | 3.44 | 287 |
| 2 | 1.93 | 4.27 | 346 | 2.00 | 2.28 | 284 |
| 4 | 1.90 | 1.33 | 338 | 2.08 | 1.85 | 282 |
| 8 | 1.77 | 1.05 | 336 | 2.01 | 1.46 | 280 |

$$z(\alpha) = \phi T^2, \tag{18}$$

where $\phi$ is the heat flow evaluated during the crystal growth represented by the following equation:

$$\phi = \Delta H_c k_0 \exp(-E/RT) f(\alpha), \tag{19}$$

and

$$f(\alpha) = n(1-\alpha)[-\ln(1-\alpha)]^{(n-1)/n}, \tag{20}$$

where $\Delta H_c$ is the enthalpy difference associated with crystallization process. Figure 2 represents the variation of $y(\alpha)$ and $z(\alpha)$ with crystallized fraction $\alpha$. As shown in the plots, the maximum of $z(\alpha)$ falls in the range (0.50–0.59) and (0.55–0.60) for Peaks 1 and 2, respectively; whereas that of $y(\alpha)$ falls in the range (0.27–0.35) and (0.38–0.45), respectively, for Peaks 1 and 2. These values are less than that predicted by Malek. Hence in the present case, KJMA model cannot be used for the study of non-isothermal crystallization kinetics.

For a more rigorous check of applicability of KJMA equation, we have obtained the theoretical normalized heat flow curves by making use of calculated kinetic parameters i.e., $E$ and $n$ and Eqs. (19) and (20). Figure 3a–h represents the experimental normalized heat flow and the theoretically calculated normalized heat flow using Eqs. (19) and (20). For isokinetic methods the values of $E$, $n$, and $k_0$ used are those obtained from the least square fitting method and are listed in Table 1. For isoconversional methods, $E$ and $k_0$ values used are calculated by KAS method. The values of local Avrami exponent are calculated using the following equation [39]:

$$n(\alpha) = -\frac{R}{E(\alpha)} \frac{\partial \ln[-\ln(1-\alpha)]}{\partial(1/T)}. \tag{21}$$

It can be seen from Fig. 3a–h that isoconversional and isokinetic methods show a close match to each other. Both of them show a deviation from the experimental data at lower heating rates. As heating rate increases, the theoretically calculated normalized heat flow values match with the experimental data. Further, for all heating rates the calculated values deviate at both the tails of the peak, but show a close match in intermediate temperature range. This deviation at the peak tails may be due to high errors in the base-line interpolation for peak tails [37]. It can also be noted that before peak crystallization temperature, the normalized heat flow calculated by isoconversional method matches more accurately with the experimental results, except for Fig. 3b. After the near-peak region, the isokinetic method provides better results. It can be understood in terms of nucleation and growth processes. During initial stages of crystallization process nucleation and growth occur simultaneously, but after the peak nucleation process becomes negligible and crystallization is dominated by growth process. Thus, the entire crystallization process is a

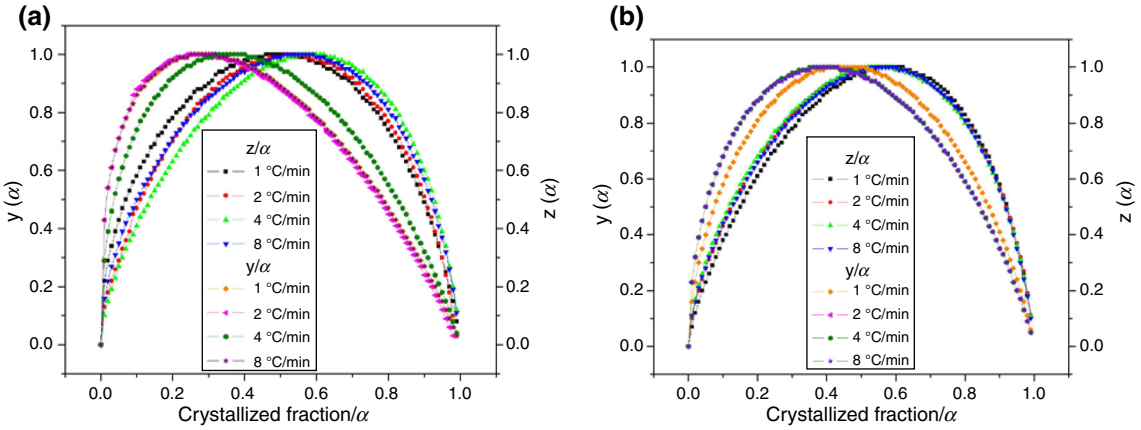


**Fig. 2** Normalized $y(\alpha)$ and $z(\alpha)$ with crystallized fraction $\alpha$ for different heating rates; **a** Peak 1 and **b** Peak 2

complex phenomenon and hence it cannot be explained completely by isokinetic methods. For understanding this complex process, the dependence of $E$ on $\alpha$ is studied by various isoconversional methods.

Linear integral isoconversional methods

*KAS method*

The expression for KAS [32, 33] method is as follows

$$\ln\left(\frac{\beta}{T_\alpha^2}\right) = -\frac{E_\alpha}{RT_\alpha} + \ln\left(\frac{k_0 R}{E_\alpha}\right). \tag{9}$$

The modified equation for non-linear heating rate is given by Eq. (11)

$$\ln\left(\frac{\beta}{T_\alpha^2}\right) - \left(\frac{A_T\omega}{2\beta}\right)^2 + \cdots = -\frac{E_\alpha}{RT_\alpha} + \ln\left(\frac{k_0 R}{E_\alpha}\right). \tag{16}$$

The values of $E_\alpha$ and the $k_0$ can be calculated for both peaks, respectively, from the slope and intercept of the plot $\ln(\beta/T_\alpha^2)$ versus $1{,}000/T_\alpha$ for constant conversion, $\alpha$ (Fig. 4a, b). The values of local activation energies, $E_\alpha$, are reported in Table 2. The factor $(A_T\omega/2\beta)^2$ on LHS of Eq. (11) is coming out to be almost constant for all heating rates. Hence, its contribution to non-linearity is negligible, which is clearly indicated by Fig. 4a, b. Typically $(A_T\omega/\beta) \approx 1$, for e.g., for $\beta = 1$ °C $\text{min}^{-1}$, $A_T = 0.16$ and $\omega = (2\pi)/p$, where $p$ is time period (=60 s; $A_T\omega/\beta) = 1$.

*Kissinger method* This method assumes reaction rate to be maximum at peak temperature ($T_p$). It is used to calculate activation energy at a constant degree of conversion, $\alpha$, i.e., at $T_\alpha = T_p$. Kissinger equation is

$$\ln\left(\frac{\beta}{T_p^2}\right) = -\frac{E}{RT_p} + \ln\left(\frac{k_0 R}{E}\right). \tag{22}$$

Kissinger equation for MDSC can be obtained by repeating Eq. (11)–(16) resulting in the final expression:

$$\ln\left(\frac{\beta}{T_p^2}\right) - \left(\frac{A_T\omega}{2\beta}\right)^2 + \cdots = -\frac{E}{RT_p} + \ln\left(\frac{k_0 R}{E}\right). \tag{23}$$

The slope and intercept the plot $\ln(\beta/T_p^2)$ versus $1{,}000/T_p$ (Fig. 5a, b) give the values of activation energy, $E$, and the pre-exponential factor, $k_0$, respectively. The values of $E$ and $k_0$ are given in Table 3.

*Augis and Bennett's method* This method is an extension of Kissinger method and it is supposed to provide accurate values of kinetic parameters. Apart from peak temperature ($T_p$) it also incorporates onset temperature of crystallization ($T_o$) [40].

$$\ln\left(\frac{\beta}{(T_p - T_o)}\right) = -\frac{E}{RT_p} + \ln(k_0). \tag{24}$$

For non-linear heating rate, on repeating steps in Eqs. (11)–(16) we get,

$$\ln\left(\frac{\beta}{(T_p - T_o)}\right) - \left(\frac{A_T\omega}{2\beta}\right)^2 + \cdots = -\frac{E}{RT_p} + \ln(k_0). \tag{25}$$

The values of $E$ and $k_0$ calculated, respectively, from the slope and intercept of the plot $\ln(\beta/(T_p - T_o))$ versus $1{,}000/T_p$ (Fig. 6a, b) are given in Table 3 for both the peaks. This method is also applicable to heterogeneous reactions.

*Boswell method* As $((T_p - T_0)/T_p) \approx 1$, Augis and Bennett methods may provide crude results. Boswell method [41], based on the following linear equation, overcomes the limitation of Augis and Bennett method.

$$\ln\frac{\beta}{T_p} = -\frac{E}{RT_p} + \text{const.} \tag{26}$$

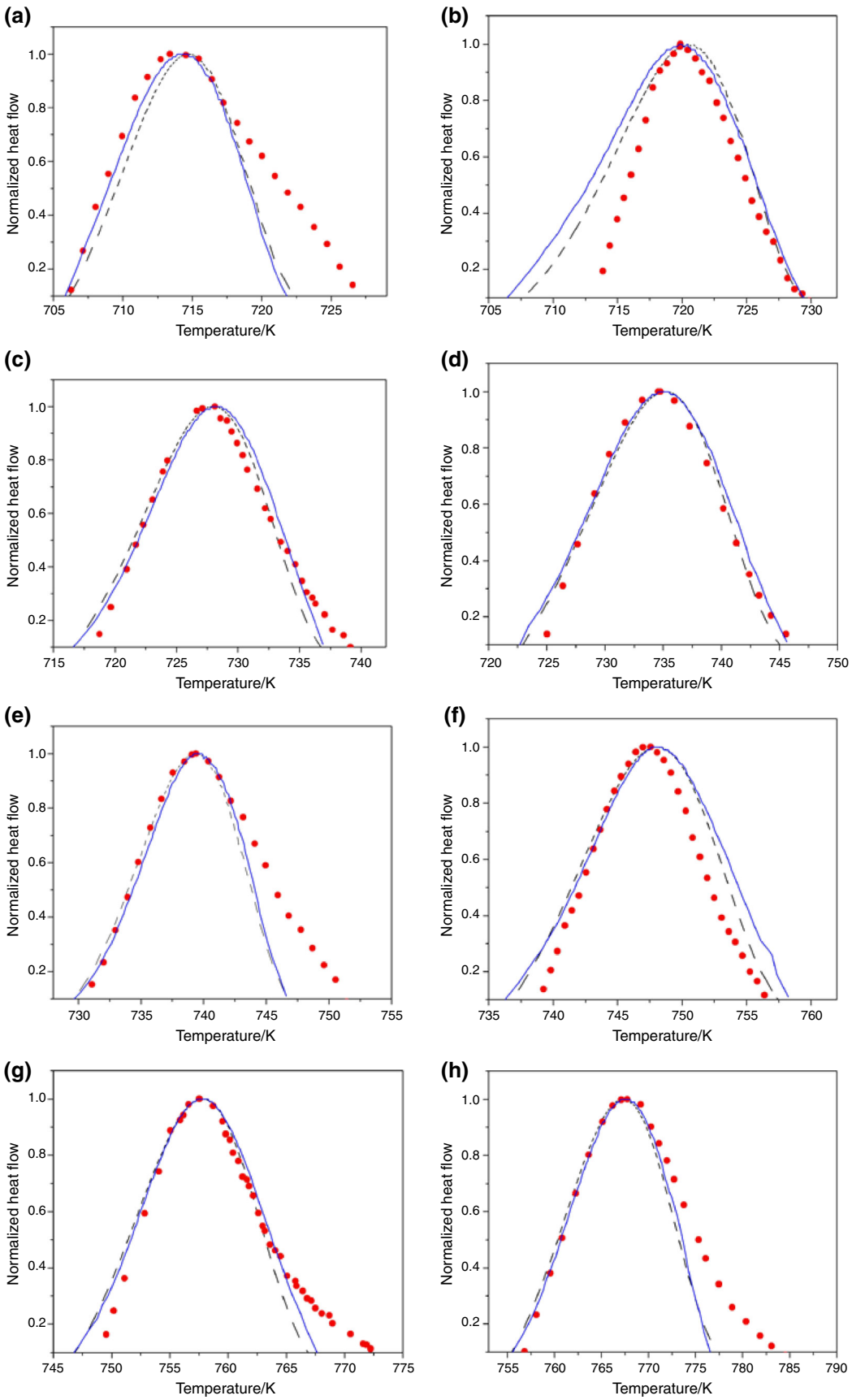

◀**Fig. 3** Normalized heat flow curves at different heating rates; (*dots*) experimental, (*dashed lines*) isokinetic results, and (*continuous lines*) isoconversional results. **a–d** Peak 1: **a** 1 °C $min^{-1}$, **b** 2 °C $min^{-1}$, **c** 4 °C $min^{-1}$, **d** 8 °C $min^{-1}$; **e–h** Peak 2: **e** 1 °C $min^{-1}$, **f** 2 °C $min^{-1}$, **g** 4 °C $min^{-1}$, **h** 8 °C $min^{-1}$

Again following Eqs. (11)–(16), for non-linear heating rate, Eq. (25) modifies to

$$\ln\frac{\beta}{T_p}-\left(\frac{A_T\omega}{2\beta}\right)^2+\cdots=-\frac{E}{RT_p}+\text{const.} \tag{27}$$

The value of $E$ as calculated from the slope of the plot $\ln(\beta/T_p)$ versus $1{,}000/T_p$ (Fig. 7a, b) is 398.24 and 324.49 kJ $mol^{-1}$, respectively, for Peaks 1 and 2. The values are given in Table 3.

*Ozawa–Flynn–Wall (OFW)* OFW [42, 43] solved Eq. (4) using Doyle's approximation [44–46]. The OFW expression is

$$\ln\beta=-1.0516\frac{E_\alpha}{RT_\alpha}+\text{const.} \tag{28}$$

Following the steps (11)–(16) for Eq. (28) we get

$$\ln(\beta)-\left(\frac{A_T\omega}{2\beta}\right)^2+\cdots=-1.0516\frac{E_\alpha}{RT_\alpha}+\text{const.} \tag{29}$$

The plot $\ln(\beta)$ versus $1{,}000/T_\alpha$ for constant conversion, $\alpha$, is shown in Fig. 8a, b for Peaks 1 and 2, respectively. The values of $E_\alpha$ are reported in Table 2. At $T_\alpha = T_p$ (Ozawa method) the value for activation energy is determined using Eq. (28), and the value is reported in Table 3 (Fig. 9a, b).

**Table 2** Local activation energies ($E_\alpha$) at different degrees of conversions, $\alpha$, for different methods

| $A$ | $E_\alpha$/kJ $mol^{-1}$ | | | | | |
|---|---|---|---|---|---|---|
| | KAS | | OFW | | Friedman | |
| | Peak 1 | Peak 2 | Peak 1 | Peak 2 | Peak 1 | Peak 2 |
| 0.1 | 418 ± 6 | 390 ± 5 | 407 ± 7 | 383 ± 5 | 420 ± 3 | 342 ± 1 |
| 0.2 | 393 ± 5 | 341 ± 4 | 383 ± 5 | 337 ± 4 | 409 ± 3 | 335 ± 1 |
| 0.3 | 559 ± 0 | 321 ± 4 | 548 ± 0 | 316 ± 7 | 403 ± 2 | 329 ± 1 |
| 0.4 | 415 ± 7 | 320 ± 4 | 407 ± 7 | 316 ± 7 | 392 ± 0 | 318 ± 1 |
| 0.5 | 418 ± 7 | 319 ± 4 | 407 ± 7 | 316 ± 4 | 417 ± 4 | 306 ± 1 |
| 0.6 | 392 ± 5 | 321 ± 4 | 383 ± 5 | 316 ± 4 | 385 ± 1 | 306 ± 1 |
| 0.7 | 433 ± 7 | 341 ± 4 | 407 ± 7 | 337 ± 4 | 369 ± 1 | 307 ± 1 |
| 0.8 | 416 ± 7 | 319 ± 4 | 407 ± 7 | 316 ± 4 | 365 ± 1 | 296 ± 2 |
| 0.9 | 392 ± 5 | 319 ± 4 | 383 ± 5 | 316 ± 4 | 355 ± 2 | 305 ± 5 |
| 1 | 390 ± 5 | 320 ± 4 | 383 ± 5 | 316 ± 4 | 304 ± 4 | 358 ± 7 |

## Linear differential isoconversional methods

These methods use the differential of the transformed fraction to calculate the activation energy, $E_\alpha$. From Eq. (6), Friedman [47] derived a linear differential isoconversional expression:

$$\ln\left(\frac{d\alpha}{dt}\right)_\alpha=\ln\beta\left(\frac{d\alpha}{dT}\right)_\alpha=-\frac{E_\alpha}{RT_\alpha}+\ln(k_0f(\alpha)). \tag{30}$$

This method is also supposed to give accurate results of $E$, since it does not apply any mathematical approximation to the temperature integral. However, since it is a differential method its accuracy is limited by signal noise.

Equation (30) can be modified to Eq. (31) by repeating Eqs. (11)–(16),

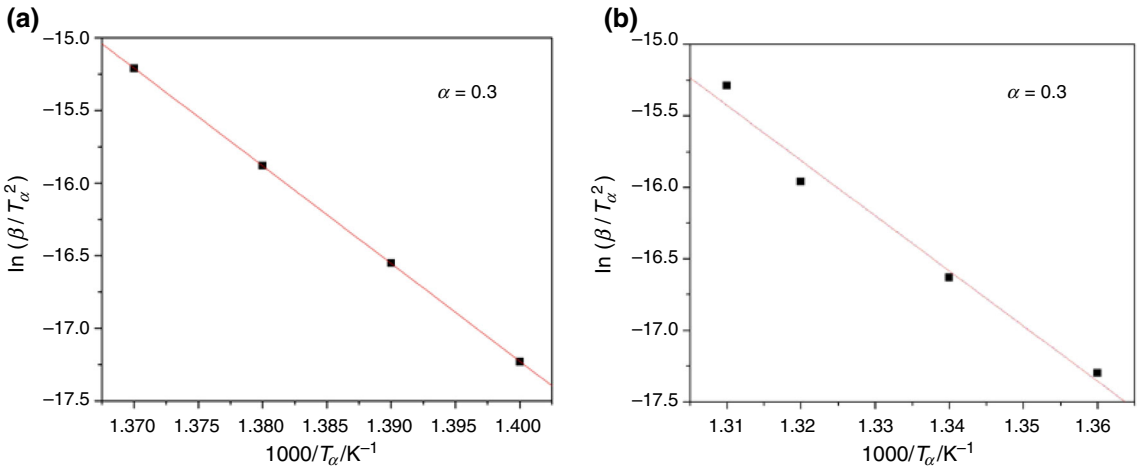


**Fig. 4** KAS plot for $\alpha = 0.3$; **a** Peak 1 and **b** Peak 2

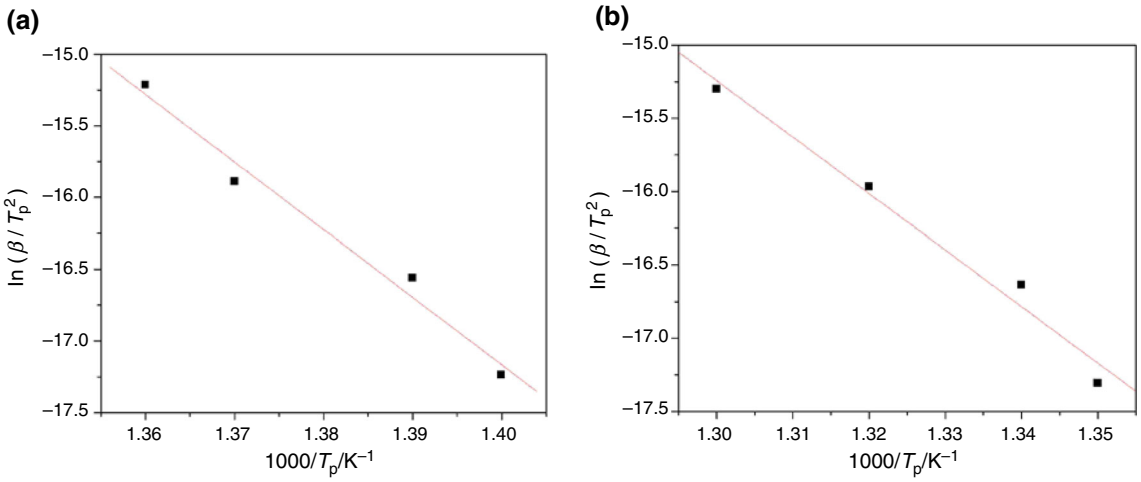


**Fig. 5** Kissinger plot; **a** Peak 1 and **b** Peak 2

**Table 3** Activation energies ($E$) and pre-exponential factor ($A$) for different methods

| Methods | $E$/kJ mol$^{-1}$ | | $k_0$/s$^{-1}$ | |
|---|---|---|---|---|
| | Peak 1 | Peak 2 | Peak 1 | Peak 2 |
| Kissinger | 392 ± 5 | 320 ± 4 | $5.67 \times 10^{22}$ | $3.93 \times 10^{16}$ |
| Augis and Bennett's method | 312 ± 9 | 282 ± 3 | $1.26 \times 10^{20}$ | $1.38 \times 10^{17}$ |
| Boswell | 398 ± 5 | 324 ± 4 | – | – |
| Ozawa | 383 ± 7 | 316 ± 5 | – | – |
| Gao and Wang | 385 ± 4 | 306 ± 1 | – | – |

$$\ln \beta \left(\frac{\mathrm{d}\alpha}{\mathrm{d}T}\right)_{\alpha} - \left(\frac{A_T \omega}{2\beta}\right)^2 + \cdots = -\frac{E_\alpha}{RT_\alpha} + \ln(k_0 f(\alpha)). \quad (31)$$

The values of $E$ can be calculated from the slope of the plot $\ln(\beta(\mathrm{d}\alpha/\mathrm{d}T)_\alpha)$ versus $1{,}000/T_\alpha$ for constant conversion, $\alpha$ (Fig. 10a, b). The values are given in Table 2.

A method suggested by Gao and Wang [48] is a special case of Friedman method. The expression used by Gao and Wang is as follows

$$\ln\left(\beta \frac{\mathrm{d}\alpha}{\mathrm{d}T_\mathrm{p}}\right) = -\frac{E}{RT_\mathrm{p}} + \text{const.} \quad (32)$$

For non-linear heating rate, again by performing steps in Eqs. (11)–(16), Eq. (32) changes to

$$\ln\left(\beta \frac{\mathrm{d}\alpha}{\mathrm{d}T_\mathrm{p}}\right) - \left(\frac{A_T \omega}{2\beta}\right)^2 + \cdots = -\frac{E}{RT_\mathrm{p}} + \text{const.} \quad (33)$$

The values of $E$ can be calculated from the slope of the plot $\ln(\beta(\mathrm{d}\alpha/\mathrm{d}T_\mathrm{p}))$ versus $1{,}000/T_\mathrm{p}$ (Fig. 11a, b). The values are given in Table 3.

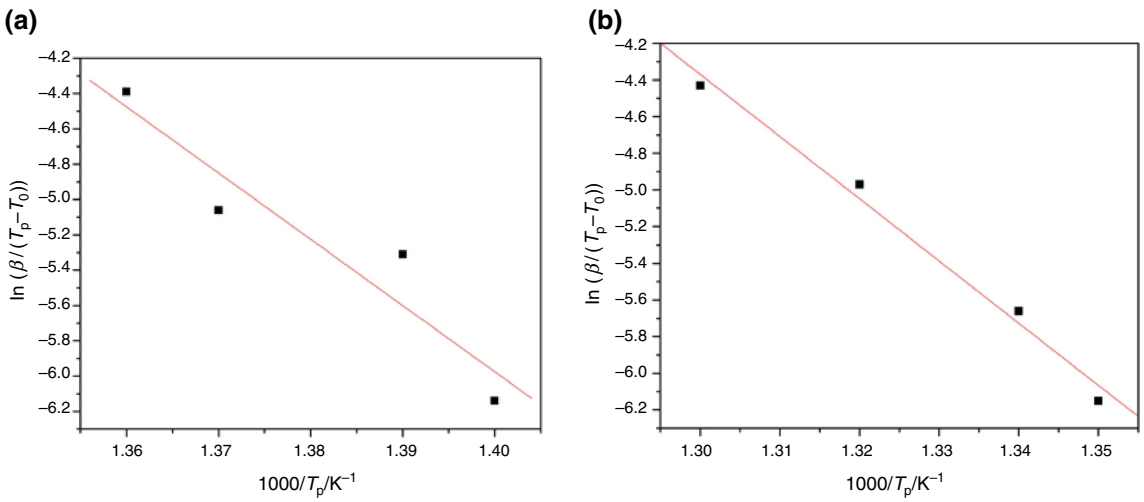


**Fig. 6** Augis and Bennett's plot; **a** Peak 1 and **b** Peak 2

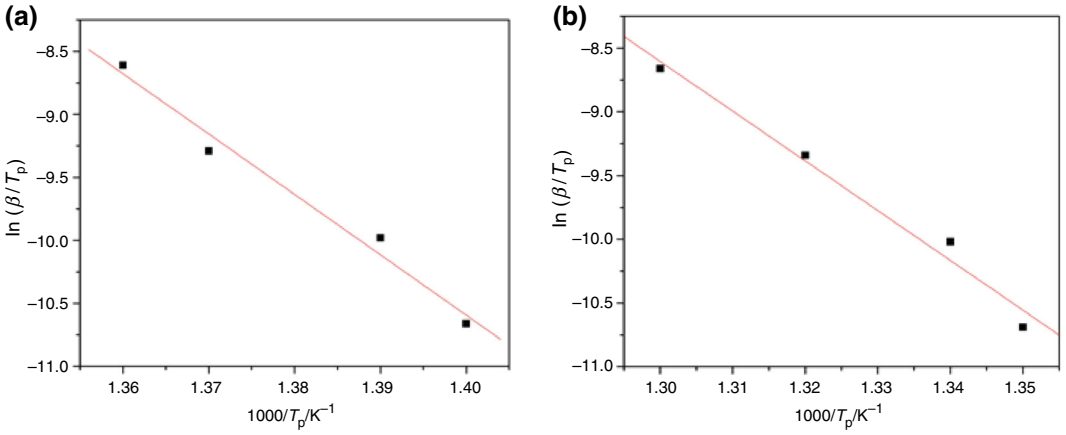


**Fig. 7** Boswell plot; **a** Peak 1 and **b** Peak 2

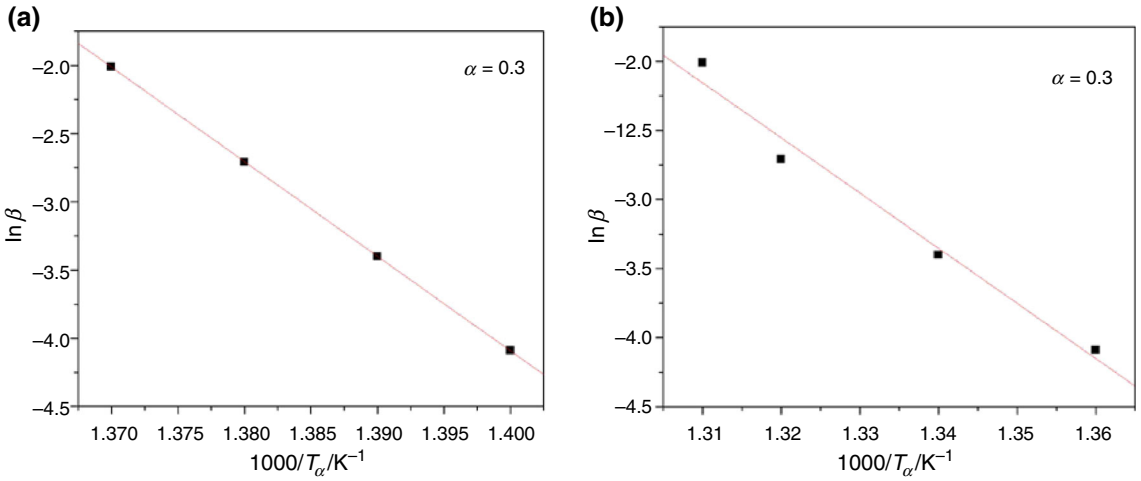


**Fig. 8** OFW plot for $\alpha = 0.3$; **a** Peak 1 and **b** Peak 2

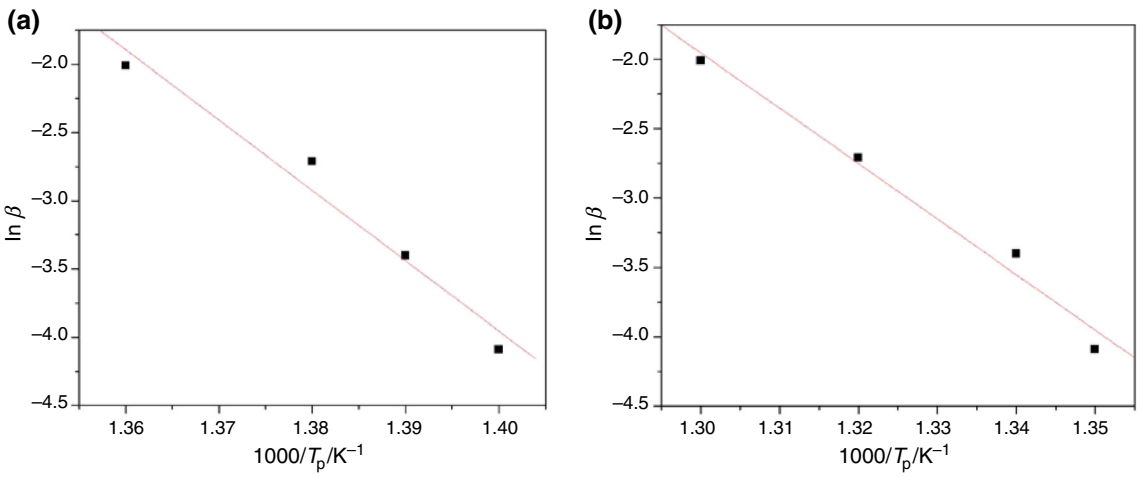


**Fig. 9** Ozawa plot; **a** Peak 1 and **b** Peak 2

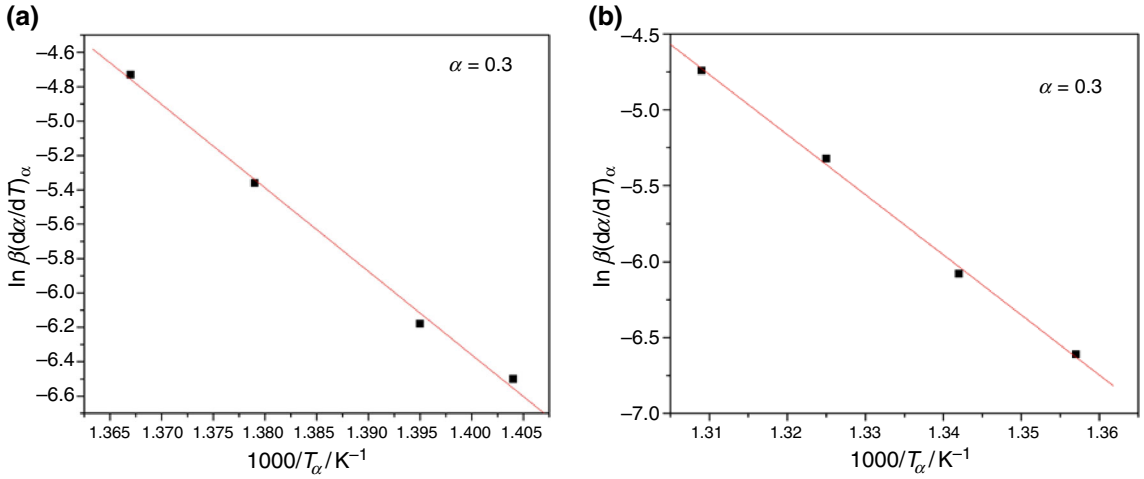


**Fig. 10** Friedman plot for α = 0.3; **a** Peak 1 and **b** Peak 2

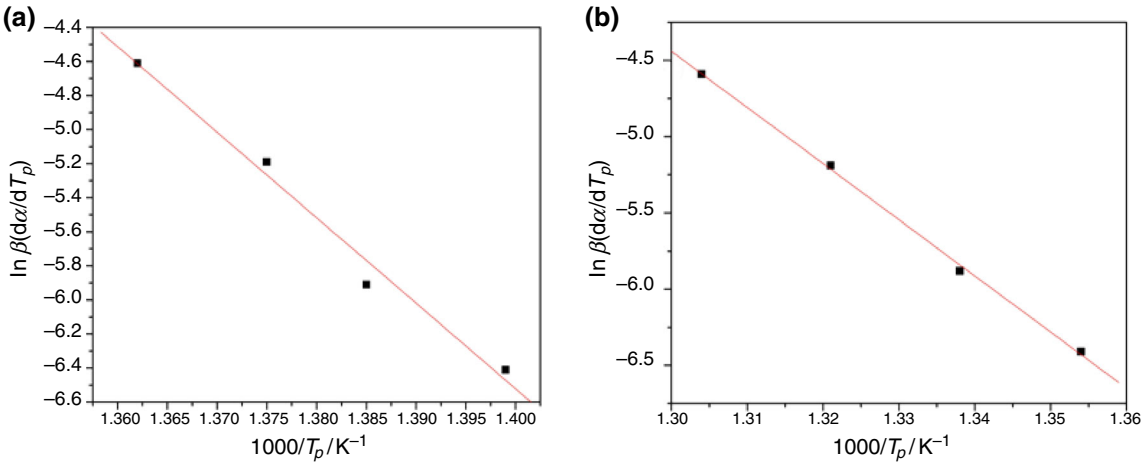


**Fig. 11** Gao and Wang plot; **a** Peak 1 and **b** Peak 2

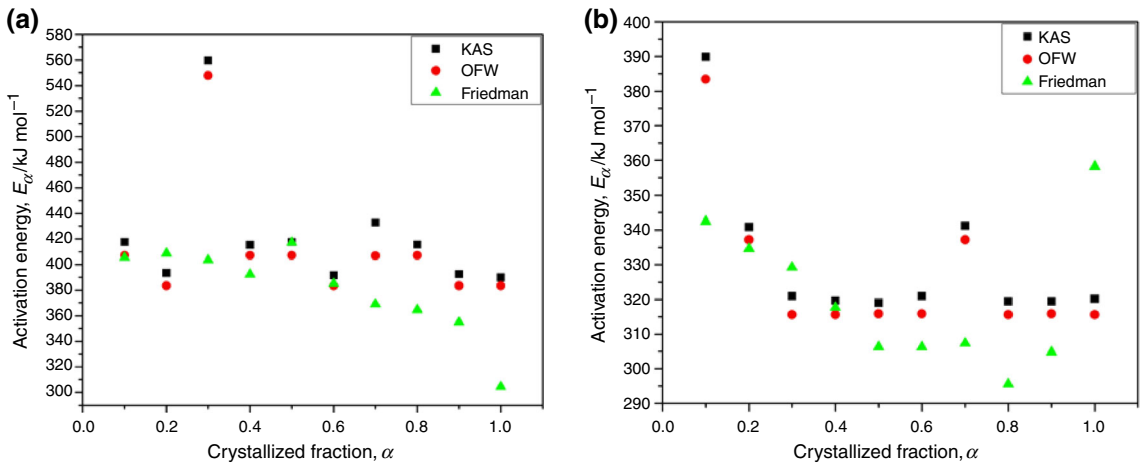


**Fig. 12** Local activation energies ($E_\alpha$) at different α from different methods; **a** Peak 1 and **b** Peak 2

The variation of local activation energies ($E_\alpha$) with the crystallized fraction, $\alpha$, has been shown in Fig. 12a, b, respectively, for Peaks 1 and 2 using three different isoconversional methods, namely KAS, OFW, and Friedman. The values of local activation energies ($E_\alpha$) at different $\alpha$ are reported in Table 2. For both the peaks KAS and OFW methods show similar variations in $E_\alpha$ with $\alpha$, provided the $E_\alpha$ values for OFW were smaller than that obtained by KAS method, whereas Friedman points varied quite differently as compared to the KAS and OFW points.

For Peak 1, all of the three methods show substantial variation with $\alpha$. KAS and OFW methods show a sudden increase in $E_\alpha$ at $\alpha = 0.3$. Then there is a decrease in $E_\alpha$ values till $\alpha = 0.6$, followed by a small increase at $\alpha = 0.7$ and then it further decreases; whereas Friedman points show a continuous decrease till end except for $\alpha = 0.5$. Therefore, the primary exothermic process can be interpreted as a multiple mechanism process. For Peak 2, $E_\alpha$ values obtained from KAS and OFW methods first decrease from $\alpha = 0.1$ to 0.3, then remain almost constant till $\alpha = 1$ except for a sudden increase at $\alpha = 0.7$. The second exothermic event can also be explained in terms of a multi-step mechanism, since $E_\alpha$ values varied considerably with $\alpha$ for all three methods.

## Conclusions

The non-isothermal crystallization kinetics for $Ti_{20}Zr_{20}Cu_{60}$ metallic glass was studied by isoconversional methods. The activation energy required for primary crystallization is found to be more than the activation energy required for subsequent crystallization peak by all the isoconversional methods. Isoconversional methods provide values of activation energy, $E_\alpha$, as a function of $\alpha$, which is not possible by any of the isokinetic methods. But the Avrami (growth) exponent that gives information about the dimensionality of crystal growth can be calculated by the use of isokinetic methods. Both methods of calculating the kinetic parameters for crystallization process provide fairly accurate results near peak crystallization temperature as seen from Fig. 3a–h. Though Fig. 1 shows that isokinetic method provides better fitting to the experimental $\alpha$ value, the complexity of crystallization event can be better understood by isoconversional methods. Hence, the combination of both methods can be used for studying the kinetics of crystallization process. KAS, OFW, and Friedman methods provide activation energies dependent on $\alpha$. The values of $E_\alpha$ obtained by KAS and OFW methods lie close to each other, whereas Friedman method shows a different variation of $E_\alpha$ with $\alpha$. For Peak 1, $E_\alpha$ values show an irregular variation with $\alpha$. For Peak 2 also there is a substantial decrease in $E_\alpha$, from $\alpha = 0.1$ to 0.3. Afterward, it remains constant except for $\alpha = 0.7$. Hence, both crystallization events are multiple mechanism processes. Also, the term that is expected to cause non-linearity, i.e., $(A_T\omega/2\beta)^2$ is almost constant for all heating rates. Thus, the non-linear heating rate does not change the nature of different linear isoconversional methods. The linear behavior of the various expressions remains intact. Hence, MDSC can be conveniently used for studying kinetics of crystallization of metallic glasses.

**Acknowledgements** The authors want to thank Institute of Material Research, Tohoku University, Sendai, Japan, for providing the sample. Sincere thanks are due to Dr. K. N. Lad for useful discussions. The authors are thankful to IUC for DAE Facility at Indore, for providing modulated DSC equipment to carry out this work. One of the authors (Supriya Kasyap) is grateful to the Department of Science and Technology (DST), Government of India, for providing financial assistance under the DST-PURSE Fellowship Scheme.

## References

1. Ligero RA, Vazquez J, Villares P, Jimenez-Garay R. Crystallization kinetics in the As–Se–Te system. Thermochim Acta. 1990;162:427–34.
2. Moharram AH, El-Oyoun MA, Abu-Sehly AA. Calorimetric study of the chalcogenide $Se_{72.5}Te_{20}Sb_{7.5}$ glass. J Phys D. 2001;34:2541–6.
3. Rysava N, Spasov T, Tichy L. Isothermal DSC methods for evaluation of the kinetics of crystallization in the Ge–Sb–S glassy system. J Therm Anal. 1987;32:1015–21.
4. Giridhar A, Mahadevan S. Studies on the As–Sb–Se glass system. J Non Cryst Solids. 1982;51:305–15.
5. Afify S. Differential scanning calorimetric study of chalcogenide glass $Se_{0.7}Te_{0.3}$. J Non Cryst Solids. 1991;128:279–84.
6. Inoue A, Zhang W, Zhang T, Kurosaka K. Thermal and mechanical properties of Cu-based Cu–Zr–Ti bulk glassy alloys. Mater Trans JIM. 2001;42:1149–51.
7. Kovneristyj YK, Pashkovskaya AG. Bulk amorphization of alloys in the intermetallide containing system Ti–Cu–Zr. Amorf (Stekloobraz) Met Mater RAN Int Metallurgii M. 1992; p.153–7.
8. Patel AT, Pratap A. kinetics of crystallization of $Zr_{52}Cu_{18}Ni_{14}Al_{10}Ti_6$ metallic glass. J Therm Anal Calorim. 2012;107:159–65.
9. Chovanee J, Chromcikova M, Pilny P, Shanelova J, Malek J, Liska M. $As_2Se_3$ melt crystallization studied by quadratic approximation of nucleation and growth rate temperature dependence. J Therm Anal Calorim. 2013;114:971–7.
10. Lad KN, Savalia RT, Pratap A, Dey GK, Banerjee S. Isokinetic and isoconversional study of crystallization kinetics of a Zr-based metallic glass. Thermochim Acta. 2008;473:74–80.
11. Abdelazim NM, Abdel-Latief AY, Abu-Sehly AA, Abdel-Rahim MA. Determination of activation energy of amorphous to crystalline transformation for $Se_{90}Te_{10}$ using isoconversional methods. J Non Cryst Solids. 2014;387:79–85.
12. Lu XC, Li HY. Kinetics of non-isothermal crystallization in $Cu_{50}Zr_{43}Al_7$ and $(Cu_{50}Zr_{43}Al_7)_{95}Be_5$ metallic glasses. J Therm Anal Calorim. 2014;115:1089–97.
13. Wu J, Pan Y, Pi J. On non-isothermal kinetics of two Cu-based bulk metallic glasses. J Therm Anal Calorim. 2014;115:267–74.
14. Svoboda R, Malek J. Is the original Kissinger equation obsolete today? J Therm Anal Calorim. 2014;115:1961–7.
15. Starnik MJ. The analysis of Al-based alloys by calorimetry quantitative analysis of reactions and reaction kinetics. Int Mater Rev. 2004;49:191–226.

16. Deb P. Ch. 1: kinetics of heterogeneous solid state processes. Berlin: Springer; 2014.
17. Kolmogorov AN. On the statistical theory of the crystallization of metals. Bull Acad Sci USSR Phys ser. 1937; 3:355–9.
18. Johnson WA, Mehl PA. Reaction kinetics of nucleation and growth. Trans Am Inst Min Metall Eng. 1939;135:416–32.
19. Avrami M. Kinetics of phase change. I: General theory. J Chem Phys. 1939;7(12):1103–12.
20. Avrami M. Kinetics of phase change. II Transformation–time relations for random distribution of nuclei. J Chem Phys. 1940;8(2):212–24.
21. Avrami M. Granulation, phase change, and microstructure kinetics of phase change III. J Chem Phys. 1941;9(2):177–84.
22. Mohan NS, Chen R. Numerical curve fitting for calculating glow parameters. J Phys D. 1970;3:243–9.
23. Tang W, Liu Y, Zhang H, Wang C. New approximation formula for Arrhenius temperature integral. Thermochim Acta. 2003;408:39–43.
24. Gorbachev VM. A solution of the exponential integral in the non-isothermal kinetics for linear heating. J Therm Anal. 1975;8:349–50.
25. Paulik F. Ch. 1: special trends in therm anal. Chichester: Wiley; 1995.
26. Vyazovkin S, Wight CA. Model-free and model-fitting approaches to kinetic analysis of isothermal and nonisothermal data. Thermochim Acta. 1999;340–341:53–68.
27. Burnham AK, Dinh LN. A comparison of isoconversional and model-fitting approaches to kinetic parameter estimation and application predictions. J Therm Anal Calorim. 2007;89(2):479–90.
28. Starnik MJ. The determination of activation energy from linear heating rate experiments: a comparison of the accuracy of isoconversion methods. Thermochim Acta. 2003;404:163–76.
29. Vyazovkin S, Dollimore D. Linear and nonlinear procedures in isoconversional computations of the activation energy of non-isothermal reactions in solids. J Chem Inf Comput Sci. 1996; 36(1):42–5.
30. Pratap A, Rao TLS, Lad KN, Dhurandhar HD. Isoconversional *vs.* Model fitting methods. J Therm Anal Calorim. 2007;89(2): 399–405.
31. Pacurariu C, Lazau I. Non-isothermal crystallization kinetics of some glass-ceramics with pyroxene structure. J Non Cryst Solids. 2012;358:3332–7.
32. Kissinger HE. Reaction kinetics in differential thermal analysis. Anal Chem. 1957;29:1702–6.
33. Akahira T, Sunose T. Joint convention of four electrical institutes. Research report (Chiba Institute of Technology). Sci Technol. 1971;16:22–31.
34. Coats AW, Redfern JP. Kinetic parameters from thermo-gravimetric data. Nature (Lond). 1964;201:68–9.
35. Pratap A, Sharma K. Applications of some thermo-analytical techniques to glasses and polymers. J Therm Anal Calorim. 2012;107(1):171–82.
36. Henderson DW. Thermal analysis of non isothermal crystallization kinetics in glass forming liquids. J Non-Cryst Solids. 1979;30:301–15.
37. Malek J. The applicability of Johnson–Mehl–Avrami model in the thermal analysis of the crystallization kinetics of glasses. Thermochim Acta. 1995;267:61–73.
38. Malek J. Kinetic analysis of crystallization processes in amorphous materials. Thermochim Acta. 200;355:239-53.
39. Lu W, Yan B, Huang W. Complex primary crystallization of amorphous finemet alloy. J Non-Cryst Solids. 2005;351:3320–4.
40. Augis A, Bennett JE. Calculation of Avrami parameters for heterogeneous solid state reactions using modification of the Kissinger method. J Therm Anal Calorim. 1978;13:283–92.
41. Boswell PG. On the calculation of activation energies using modified Kissinger method. J Therm Anal Calorim. 1980;18: 353–8.
42. Ozawa T. Anew method for analyzing thermogravimetric data. Bull Chem Soc Jpn. 1965;38:1881–6.
43. Flynn JH, Wall LA. General treatment of the thermogravimetry of polymers. J Res Natl Bur Stand A. 1966;70A:487–523.
44. Doyle CD. Kinetic analysis of thermogravimetric data. J Appl Polym Sci. 1961;5:285–92.
45. Doyle CD. Estimating isothermal life from thermogravimetric data. J Appl Polym Sci. 1962;6:642–93.
46. Doyle CD. Series approximation to the equation of thermogravimetric data. Nature (Lond.). 1965;207:290–1.
47. Friedman HL. Kinetics of thermal degradation of char-forming plastics from thermogravimetry. J Polym Sci. 1964;C6:183–95.
48. Gao YQ, Wang W. On the activation energy of crystallization in metallic glasses. J Non Cryst Solids. 1986;81:129–34.

# Effect of micro alloying on glass forming ability of Cu50Zr50 metallic glass

Supriya Kasyap, Ashmi T. Patel, and Arun Pratap

Citation: AIP Conf. Proc. **1536**, 651 (2013); doi: 10.1063/1.4810395
View online: http://dx.doi.org/10.1063/1.4810395
View Table of Contents: http://proceedings.aip.org/dbt/dbt.jsp?KEY=APCPCS&Volume=1536&Issue=1
Published by the American Institute of Physics.

# Effect of Micro Alloying on Glass Forming Ability of $Cu_{50}$ $Zr_{50}$ Metallic Glass

Supriya Kasyap, Ashmi T. Patel, Arun Pratap

*Condensed Matter Physics Laboratory, Applied Physics Department, Faculty of Technology and Engineering, The Maharaja Sayajirao University of Baroda, Vadodara -390 001, India*

**Abstract.** The sensitivity of glass forming ability (GFA) of $Cu_{50}Zr_{50}$ metallic glass towards addition of Nb and Al has been studied. It has been found that the GFA of $Cu_{50}Zr_{50}$ ribbons increases with addition of Nb and Al, and highest GFA is achieved at 4% Al. Moreover Al addition favors the formation of Bulk Metallic Glasses (BMG). Among various GFA parameters ($\Delta G$, $T_{rg}$ , $\gamma$ , $\gamma_m$ , $\eta$ , $\Delta T_x$ , Q) , it is the Gibbs free energy difference ($\Delta G$), between the under cooled liquid and the corresponding crystalline phase, that best explains this variation in GFA.

**Keywords:** .Glass forming ability (GFA), Bulk metallic glasses (BMG), Gibbs free energy difference ($\Delta G$).
**PACS:** 64.70. P-, 64.70. pe, 64.70.Q- , 64.70.qd

## INTRODUCTION

The information about the GFA has an important place in study of BMGs as it gives a clear indication about mechanism of glass formation, which thereby provides a better design of new BMG. The empirical rules given by Inoue et al. [1] and Johnson [2] have significantly contributed to the understanding of GFA of BMG, with some exceptions [3]. Cu-Zr binary alloys are among those exceptions. The alloy $Cu_{50}Zr_{50}$ is one of the best glass formers in Cu-Zr systems [3]. Furthermore, partial substitution of alloying elements to binary alloys improves their GFA significantly.

In present study, we have investigated effect of Nb, and Al substitution on GFA of $Cu_{50}Zr_{50}$ binary alloy. Further the difference in Gibbs free energy ($\Delta G$) between the liquid phase and the corresponding crystalline phase was calculated and compared with other parameters.

## THEORETICAL FORMULATION

### Gibb's Free Energy

The Gibbs free energy difference ($\Delta G$) between liquid and corresponding crystalline phase is given by

$$\Delta G = \Delta H - T\Delta S \quad (1)$$

Where, $$\Delta H = \Delta H_m - \int_T^{T_m} \Delta C_p dT \quad (2)$$

And $$\Delta S = \Delta S_m - \int_T^{T_m} \Delta C_p \frac{dT}{T} \quad (3)$$

where, $\Delta S_m$, $\Delta H_m$ and $T_m$ are the entropy, enthalpy and temperature of fusion, respectively. They are related to each other by the relation: $\Delta S_m = \Delta H_m / T_m$ (4)

$\Delta C_p$, defined as $C_p^l - C_p^x$, is the difference in specific heats of liquid and corresponding crystalline phase. If the experimental specific heat data is available for under cooled and crystal phases, then experimental $\Delta G$ can be calculated using Eq. (1)-(3). But in absence of experimental data we have to switch to approximations i.e., expressing temperature dependence of $\Delta C_p$ in a suitable way. Plenty of approximations have been done to derive expressions of $\Delta G$ [4-9]. Turnbull [7] assumed $\Delta C_p = 0$ thereby giving: $\Delta G = \Delta H_m \Delta T / T_m$ (5)

Lad et al. [8] assumed $\Delta C_p = \Delta H_m / T_m$ and used Taylor series expansion of $\ln(T_m/T) = \ln(1+\Delta T/T) = \Delta T[1 - \Delta T/2T ] / T$, retaining terms upto second order and derived the expression:

$$\Delta G = \frac{\Delta H_m \Delta T}{T_m}\left(1 - \frac{\Delta T}{2T}\right) \quad (6)$$

Again, considering Taylor series expansion of $\ln(T_m/T) = \ln (1 + \Delta T/ (Tm+T)/2)$ and retaining up to second order terms i.e, $\ln(Tm/T) = 4T\Delta T / (T_m+T)^2$ Lad et al. [9] gave the expression:

$$\Delta G = \frac{\Delta H_m \Delta T}{T_m}\left(\frac{4T^2}{\left(T + T_m\right)^2}\right) \quad (7)$$

## RESULTS AND DISSCUSSION

### Glass Forming Ability

Suppression of nucleation and growth from an under cooled melt is essentially required for glass formation. Based on $T_g$, $T_x$, & $T_m$, many parameters have been proposed in literature [10], for predicting the glass forming ability. The most frequently used parameters are the reduced glass transition

*Proceeding of International Conference on Recent Trends in Applied Physics and Material Science*
AIP Conf. Proc. 1536, 651-652 (2013); doi: 10.1063/1.4810395

temperature, $T_{rg}$, super cooled liquid range $\Delta T_x$, and parameter γ. Table 1 reports various GFA parameters for $Cu_{50}Zr_{50}$, $Cu_{48}Zr_{48}Nb_4$, and $Cu_{48}Zr_{48}Al_4$ alloys. Low values of η and ΔG indicates high GFA. On the contrary, other parameters, $\Delta T_x$, $T_{rg}$, γ $\gamma_m$, α, δ, show high values for good glass formers. It is evident from the table 1, that Nb and Al addition improves the glass forming ability. As far as ribbons are concerned almost all parameters give an appropriate variation with GFA. However, most of them are unable to explain the GFA variation of $(Cu_{50}Zr_{50})_{96}Al_4$ alloy as thickness increases, but Q factor and η satisfactorily explain this variation. Q factor is greatest for $(Cu_{50}Zr_{50})_{96}Al_4$ ribbon and decreases as thickness increases, whereas η is smallest for ribbon and increases with thickness. ΔG (Tg) varies significantly for different compositions. ΔG, which is the driving force of nucleation, is one of the dominating factors that affect kinetics of crystallization. A lower value of ΔG implies greater GFA. It can be seen that ΔG for $(Cu_{50}Zr_{50})_{96}Nb_4$ is less than that of $Cu_{50}Zr_{50}$, and is lowest for $(Cu_{50}Zr_{50})_{96}Al_4$ alloy, it indicates that among the three metallic alloys $(Cu_{50}Zr_{50})_{96}Al_4$ is the best glass former.

**TABLE 1.** GFA parameters : $T_x$ =crystallization temperature, $T_g$ = glass transition temperature, $T_l$ = liquidus temperature, $H_m$ = enthalpy of melting, $H_x$ = enthalpy of crystallization.

| **Compositions** | **$\Delta T_x$ (K)** [11] | **$T_{rg}$ ($T_g/T_l$)** [11] | **$\gamma$** [11] **($T_x/(T_g+T_l)$)** | **$\gamma_m$ ($(2T_x-T_g)/T_l$)** | **Q ($(Tg+Tx)/Tl$) ($\Delta Hx/\Delta Hm$)** | **η (1-($\Delta Hx/\Delta Hm$))** | **α (Tx/Tl)** | **δ ($T_x/(T_l-T_g)$)** | **ΔG (kJ/mol)** |
|---|---|---|---|---|---|---|---|---|---|
| **$Cu_{50}Zr_{50}$** (ribbon) | 50 | 0.57 | 0.39 | 0.65 | 0.64 | 0.46 | 0.61 | 1.43 | 1.69 |
| **$(Cu_{50}Zr_{50})_{96}Nb_4$** (ribbon) | 50 | 0.58 | 0.39 | 0.66 | 0.68 | 0.42 | 0.62 | 1.45 | 1.64 |
| **$(Cu_{50}Zr_{50})_{96}Al_4$** (ribbon) | 51 | 0.59 | 0.40 | 0.67 | 0.77 | 0.37 | 0.63 | 1.53 | 1.42 |
| **$(Cu_{50}Zr_{50})_{96}Al_4$** (2mm) | 48 | 0.59 | 0.40 | 0.67 | 0.75 | 0.38 | 0.63 | 1.52 | 1.42 |
| **$(Cu_{50}Zr_{50})_{96}Al_4$** (4mm) | 49 | 0.59 | 0.40 | 0.67 | 0.69 | 0.43 | 0.63 | 1.52 | 1.42 |
| **$(Cu_{50}Zr_{50})_{96}Al_4$** (6mm) | 50 | 0.59 | 0.40 | 0.67 | 0.52 | 0.57 | 0.63 | 1.52 | 1.42 |

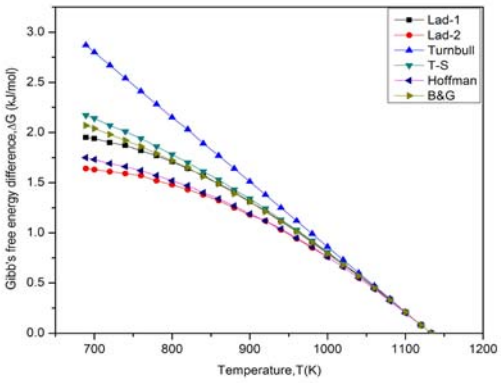


**FIGURE 1.** Variation of Gibb's free energy difference with temperature, for $Cu_{48}Zr_{48}Al_4$ alloy.

The variation of ΔG between glass transition temperature ($T_g$) and melting temperature ($T_m$) have been shown in fig. 1. for $Cu_{48}Zr_{48}Al_4$ alloys. The plot clearly indicates that the value of ΔG at $T_g$, obtained by Eq. (6) and (7) are lowest as compared to that obtained by other expressions. Further, as the under-cooled region (ΔT) increases, the nonlinearity in ΔG can be better explained by Eq. (6) & (7).

## CONCLUSION

Glass forming ability of $Cu_{50}Zr_{50}$ was investigated on addition of minor alloying elements Nb and Al. It is observed that 4% of Nb addition enhances the GFA of $Cu_{50}Zr_{50}$, which is further improved by 4% of Al addition. ΔG value for $Cu_{48}Zr_{48}Al_4$ is lowest that indicate that $Cu_{48}Zr_{48}Al_4$ is the best glass former. The driving force of crystallization has been calculated by various methods available in literature. Expressions given by Lad et al. provide lower ΔG values than other expressions, which prove its reliability over others.

## REFERENCES


1. A. Inoue, A. Takeuchi, and T. Zhang: *Metall. Mater. Trans,* 29A, (1998), 1779
2. Jonson, W. L: *MRS Bulletin*. Vol. 24, No. 10, (October 1999), 42-56.
3. L. Xia, S. S. Fang, Q. Wang, Y. D. Dong &, C.T. Liu: *Applied Physic Letters*, Vol. 88, No. 17, (April 2006), 171905-171905-3
4. J.D. Hoffman: *J. Chem. Phys*. 29 (1958), 1192
5. C.V. Thompson, F. Spaepen: *Acta Metall*. 27 (1979), 1855.
6. L. Battezatti and E. Garonne: *Z. Metallk*. 75 (1984), 305.
7. D. Turnbull: *Contem. Phys. Vol*. 10 (1969), 473.
8. K. N. Lad, A. Pratap, K. G. Raval *: J. Mater. Sci. Lett*. Vol. 21(2002) 1419
9. K. N. Lad, K. G. Raval, A. Pratap*: J. Non-Cryst. Solids* Vol. 334&335 (2004) 259.
10. Sheng Guo , Z.P. Lu, C.T. Liu*: Intermetallics* 18 (2010) 883–888.
11. T. A. Baser & M. Baricco: *Rev. Adv. Mater. Sci*. 18 (2008), 71-76.

# Glass Forming Ability of Zr-based Amorphous Alloys

Supriya Kasyap,[a] Sonal R. Prajapati,[a] and Arun Pratap,[a,*]
[a]*Condensed Matter Physics Laboratory, Applied Physics Department, Faculty of Technology and Engineering, The Maharaja Sayajirao University of Baroda, Vadodara -390 001, India*
*apratapmsu@yahoo.com

**Received: 15/02/2016 Accepted: 20/04/2016**

The glass forming ability (GFA) of five Zr-based alloys, namely $Zr_{62.5}Al_{12.1}Cu_{7.95}Ni_{17.45}$, $Zr_{63}Al_{11.4}Cu_{9.3}Ni_{16.3}$, $Zr_{63.5}Al_{10.7}Cu_{10.7}Ni_{15.1}$, $Zr_{64}Al_{10.1}Cu_{11.7}Ni_{14.2}$, and $Zr_{65}Al_{8.7}Cu_{14.4}Ni_{11.9}$, is studied based on the thermodynamic parameter i.e., the Gibbs free energy difference ($\Delta G(T_g)$) between the super-cooled liquid and the corresponding crystalline phase. Two different equations of $\Delta G$, given by Lad et al, are used and the calculated values of $\Delta G(T_g)$ are plotted against the critical dimension ($Z_{max}$) to understand the relationship between the GFA and $\Delta G(T_g)$. It is found that $\Delta G(T_g)$ obtained by Lad-1 expression, shows a strong correlation with $Z_{max}$ ($R^2 = 0.955$). Other GFA parameters ($\gamma_m$, $\alpha$, $\delta$, $\xi$, $\Phi$, $\omega$, $\omega_2$, $\omega'$, $\beta$, $\beta'$, etc) are also calculated to understand the glass forming ability and thermal stability of metallic glasses. Among all five compositions, $Zr_{62.5}Al_{12.1}Cu_{7.95}Ni_{17.45}$ is found to have the best glass forming ability with $\Delta G(T_g)$ values to be 5.166 and 4.359 $kJmol^{-1}$ respectively by Lad-1 and Lad-2 expression.

**Keywords:** Glass Forming Ability (GFA), Gibbs free energy difference ($\Delta G$), critical dimension ($Z_{max}$)

## 1. Introduction

The unavailability of appropriate number of crystal nucleation sites is the chief reason behind the formation of a glass from a metallic melt during its cooling process. Crystal nucleation is favored by a large thermodynamic driving force and a rapid kinetics of crystal nucleation. As soon as a metallic alloy is cooled, its molecules either tend to move towards their equilibrium state or get supercooled, depending on the amount of the thermodynamic driving force available and the briskness of crystallization kinetics. The thermodynamic driving force can be determined by calculating the Gibbs free energy difference ($\Delta G$) between the supercooled liquid and the corresponding crystalline phase.

The glass forming ability (GFA) of metallic alloy primarily depends on its cooling rate. As cooling rate increases, the relaxation time decreases. Hence, molecules of alloy do not get sufficient time to move to their respective equilibrium places and supercooling of a melt takes place. This implies that high cooling rate favors good glass formability. But in practice, many researchers have reported their work on formation of metallic glasses even at lower cooling rates [1-4]. The critical cooling rate ($R_c$) i.e., the minimum cooling rate that allows the formation of fully amorphous material from a metallic melt, is an important experimental factor that determine the GFA of a metallic glass. The maximum attainable size of a fully amorphous alloy i.e., the critical dimension ($Z_{max}$) of a metallic glass is another factor that is useful in determining the GFA of a metallic glass. A greater $Z_{max}$ indicates a better ability of an amorphous alloy to form a bulk metallic glass (BMG). Apart from these experimental

parameters, a large number of quantitative parameters are available in literature [5-17] for studying the GFA of BMGs. However, there are not many studies on the relationship between the quantitative GFA parameters and the experimentally measured parameters i.e., $R_c$ and $Z_{max}$. Identification of the best GFA parameter is vital for finding the best glass former. Hence the correlation between the GFA parameters and $R_c$ (or $Z_{max}$) is essential for better understanding of the GFA of amorphous alloys.

In present work, we have studied the GFA of five Zr-based metallic glasses i.e., $Zr_{62.5}Al_{12.1}Cu_{7.95}Ni_{17.45}$, $Zr_{63}Al_{11.4}Cu_{9.3}Ni_{16.3}$, $Zr_{63.5}Al_{10.7}Cu_{10.7}Ni_{15.1}$, $Zr_{64}Al_{10.1}Cu_{11.7}Ni_{14.2}$, and $Zr_{65}Al_{8.7}Cu_{14.4}Ni_{11.9}$. Various GFA parameters together with the thermodynamic parameter $\Delta G$ ($T_g$) have been evaluated and their relationship with $Z_{max}$ is studied for Zr-based metallic glasses.

## 2. Theory

The glass forming ability and glass stability of metallic glasses can be studied theoretically by making use of the available GFA parameters such as, $\Delta T_x$[= $T_x$-$T_g$] [1], $T_{rg}$[= $T_g/T_l$] [5], $\gamma$[=$T_x/(T_g+T_l)$] [6], $\beta'$[= $T_xT_g/(T_l-T_x)^2$] [7], $\delta$[= $T_x/(T_l - T_g)$] [8], $\gamma_m$[= $(2T_x-T_g)/T_l$] [9], $\alpha$[= $T_x/T_l$] [10], $\beta$[= $T_x/T_g$ - $T_g/T_l$] [10], $\zeta$[=$T_g/T_l$ - $\Delta T_x/T_x$] [11], $\omega'$[= $(T_g/T_x)$ - $(2T_g/(T_g+T_l))$] [12], $\omega_2$[=$T_g/(2T_x - T_g) - (T_g/T_l)$] [13], $\varphi$[= $T_{rg}$ $(\Delta T_x/T_g)^{0.143}$] [14], $\gamma_c$[= $(3T_x-2T_g)/T_l$] [15], $\omega$[=$T_l(T_l + T_x) / T_x(T_l - T_x)$] [16], and $\Delta T_{rg}$[= $(T_x-T_g)/(T_l-T_g)$] [17]. Here, $T_g$, $T_x$, and $T_l$ are the glass transition temperature, crystallization temperature and liquidus temperature respectively.

The Gibbs free energy difference ($\Delta G$) between liquid and corresponding crystalline phase is given by

$$\Delta G = \Delta H - T\Delta S \tag{1}$$

Where,
$$\Delta H = \Delta H_m - \int_T^{T_m} \Delta C_p dT \tag{2}$$

And,
$$\Delta S = \Delta S_m - \int_T^{T_m} \Delta C_p \frac{dT}{T} \tag{3}$$

where, $\Delta S_m$, $\Delta H_m$ and $T_m$ are the entropy, enthalpy and temperature of fusion, respectively. The relation between them is: $\Delta S_m = \Delta H_m / T_m$ (4)

$\Delta C_p$, defined as $C_p^l$ - $C_p^x$, is the difference in specific heats of liquid and corresponding crystalline phase. Eq. (1)-(3) can be used to calculate experimental $\Delta G$ if the experimental specific heat data is available for under cooled and crystal phases. But in absence of experimental data, certain approximations have to be used for expressing the temperature dependence of $\Delta C_p$ in a suitable way. Plenty of approximations have been done to derive expressions of $\Delta G$ [18-22]. Lad et al. [21] assumed $\Delta C_p = \Delta C_p^m$, where $\Delta C_p^m$ is the value of $\Delta C_p$ at $T_m$, and used Taylor series expansion of $\ln(T_m/T) = (\Delta T/T)$ [1 - $\Delta T/2T$] retaining terms upto second order and derived the expression (Lad-1):

$$\Delta G = \frac{\Delta H_m \Delta T}{T_m}\left(1 - \frac{\Delta T}{2T}\right) \quad (5)$$

where, $\Delta T = T_m - T$. $\Delta T$ is the under-cooling of the metallic melt, which provides information about how far is the system from melting temperature.

Again, considering Taylor series expansion of $\ln(T_m/T)$, and retaining up to second order terms i.e, $\ln(T_m/T) = 4T\Delta T / (T_m+T)^2$ Lad et al,[22] gave the expression (Lad-2):

$$\Delta G = \frac{\Delta H_m \Delta T}{T_m}\left(\frac{4T^2}{\left(T + T_m\right)^2}\right) \quad (6)$$

## 3. Results and Discussion

The information about the glass forming ability of metallic glasses can be procured by knowledge of the experimental parameter $R_c$ i.e., the critical cooling rate. $R_c$ can be understood in terms of the minimum cooling rate sufficient enough to avoid the formation of any undesired phase, which in case of metallic glasses is the crystalline phase. A greater value of $R_c$ implies that the system requires a high cooling rate for suppressing the crystallization event, and hence lower is the glass forming ability. Experimentally, $R_c$ is considered to be the best GFA criteria. Another experimental parameter is critical dimension, $Z_{max}$. $Z_{max}$ is the maximum attainable size of fully amorphous material, which decreases with an increase in $R_c$ [23]. This implies that a good glass former will have a larger value of $Z_{max}$ as compared to a poor glass former. But determination of $R_c$ (or $Z_{max}$) involves a series of continuous cooling experiments, which itself is a tedious job. So, in order to make the work easier a variety of GFA parameters have been formulated by researchers [5-17], depending on the characteristic temperatures, such as the glass transition temperature ($T_g$), the crystallization temperature ($T_x$), the melting and liquidus temperature ($T_m$ and $T_l$ respectively). Table I represents the melting enthalpy ($\Delta H_m$), Critical dimension ($Z_{max}$), glass transition temperature ($T_g$), crystallization temperature ($T_x$), melting temperature ($T_m$), and Gibbs free energy difference at $T_g$ as calculated by expressions given by Lad et al (eq. 5 & 6).

The ability of a liquid to resist crystallization during cooling process, and hence to get supercooled into a state of rigidity, is considered as the glass forming ability. Further, the thermal stability of the liquid phase upon cooling assists the progress of the formation of glassy state. Among various available GFA parameters, the reduced glass transition temperature ($T_{rg}$) [5] and the supercooled liquid region ($\Delta T_x$) [1] are the most widely used ones. $T_{rg}$ is defined as the ratio of glass transition temperature ($T_g$) and liquidus temperature ($T_l$). Higher $T_{rg}$ values indicate good glass forming ability. The value of $T_{rg}$ is found to be in the range 0.66-0.69 for good glass formers. Here, in the case of Zr-based metallic glasses $T_{rg}$ varies from 0.55-0.57. $Zr_{63.5}Al_{10.7}Cu_{10.7}Ni_{15.1}$ metallic glass with $T_{rg}$ = 0.565 is a better glass former than $Zr_{64}Al_{10.1}Cu_{11.7}Ni_{14.2}$ with $T_{rg}$ 0.568. Hence, $T_{rg}$ does not provide correct information about the variation of GFA in Zr- based metallic glasses. $\Delta T_x$ can be understood as the difference between the $T_x$ and $T_g$. Large difference between $T_x$ and $T_g$ indicates that the material takes more time to crystallize, thereby showing better stability against crystallization. $\Delta T_x$ indicates the stability of supercooled liquid against crystallization. Generally, glass formers are supposed to have values of $\Delta T_x$ to be in the range 16.3-117. Cai

et al [24] have shown that these two parameters ($T_{rg}$ and $\Delta T_x$) cannot be used for studying the GFA of Zr-based metallic glasses, since they do not vary linearly with $Z_{max}$. Another GFA indicator $\gamma$ proposed by Li and Liu [6] is one of the good indicators of GFA with values ranging between 0.35-0.50 for good glass formers. In present case, $Zr_{62.5}Al_{12.1}Cu_{7.95}Ni_{17.45}$ is found to the best glass former ($\gamma$ = 0.40) among all the five compositions. Furthermore, the parameters $\beta'$ [7] and $\delta$ [8] were proposed depending on the classical nucleation and growth theory. Both of these parameters show a linear variation with $Z_{max}$ as observed form figure 1(a). Several other GFA indicating criterion, such as $\gamma_m$ [9], $\alpha$ [10], $\beta$ [10], $\xi$ [11], and $\omega'$ [12], $\omega_2$ [13], based on the stability of liquid phase against competing crystalline phase and the resistance of amorphous phase against crystallization, have been formulated by various researchers in the past. The parameter $\alpha$ is supposed to be applicable for studying the GFA of metallic glasses where a distinct $T_g$ is not observed [10]. The relationship of $\gamma_m$, $\alpha$, $\beta$, $\xi$, $\omega'$, and $\omega_2$ with $Z_{max}$ is shown in figures 1(a-c). Extending the applicability of GFA criterions from metallic glasses to network and molecular glasses, Fan et al [14] proposed a criterion namely $\varphi$ based on the concepts of nucleation theory and fragility. Depending upon the relation between cooling and heating process, Guo and Liu [15] formulated another GFA parameter $\gamma_c$. Fig 1 (d) represents the relation of $\varphi$ and $\gamma_c$ with $Z_{max}$. Based on the Gibbs free energy difference between the supercooled liquid phase and the corresponding crystalline phase, Ji and Pan [16] formulated thermodynamic parameter $\omega$, for evaluation of GFA of metallic glasses and oxide glasses. This parameter $\omega$ also shows a positive correlation with $Z_{max}$ (Fig. 1(e)). The variation of the reduced supercooled region ($\Delta T_{rg}$) [17] with $Z_{max}$ is shown in fig 1(f). $R^2$ value for $\Delta T_{rg}$-$Z_{max}$ plot is 0.67, which indicates that $\Delta T_{rg}$ is not an appropriate parameter for studying GFA of Zr-based metallic glasses. All the GFA parameters explain the glass forming ability of Zr-based metallic glasses satisfactorily, except for $T_{rg}$, $\Delta T_x$, and $\Delta T_{rg}$.

The thermodynamic parameter $\Delta G$ ($T_g$) is calculated by using equation (5) and (6). All the aforementioned parameters were correlated with $Z_{max}$, for identifying the best GFA parameter. Figures 1 (a) to 1 (f) represents the variation of various GFA parameters with $Z_{max}$. The parameters $\omega_2$, $\omega'$, and $\Delta G$ ($T_g$), shows a negative correlation with $Z_{max}$, whereas all other parameters show a positive correlation with $Z_{max}$. Among all GFA parameters $\Delta G$ ($T_g$) is found to have the best correlation with $Z_{max}$ (fig 2(a)), with the value of correlation coefficient $R^2$ = 0.955 and 0.944, calculated by expressions given by Lad et al (eq 5 & 6 respectively). Therefore $\Delta G$ ($T_g$) values can be used as an estimate for GFA of Zr-based metallic glasses. Among the two expressions of $\Delta G$ Lad-1 (eq 5) is found to have better linear fit with $Z_{max}$ as compared to Lad-2 expression (eq 6) as evident from fig 2(a). This indicates that Lad-1 expression provides better one-to-one correspondence of $\Delta G$ ($T_g$) values with $Z_{max}$ than Lad-2 expression. Hence for Zr-based metallic glasses Lad-1 expression for calculation of $\Delta G$ ($T_g$) explains the GFA better than eq 6.

All other GFA parameters are also showing good correlation with $Z_{max}$ with values of $R^2$ ranging from 0.8 to 0.95, except for $\Delta T_x$, $T_{rg}$, and $\Delta T_{rg}$. Moreover, Cai et al [24] found that $\Delta H_m$ can also be considered as a good GFA parameter as it varies linearly with $Z_{max}$ with $R^2$ = 0.98. It implies that along with $\Delta G$ ($T_g$), $\Delta H_m$ can also be used as a decisive criterion for GFA of metallic glasses. Further the ratio $\Delta G$ ($T_g$)/$\Delta H_m$ is found to have a nearly constant value for

a single expression of $\Delta G$. Considering equation (5) and (6), the value of $\Delta G$ ($T_g$) / $\Delta H_m$ comes out to be 0.27 and 0.22 respectively [fig.2 (b)].

The best glass former among the five Zr-based metallic glasses is found to be $Zr_{62.5}Al_{12.1}Cu_{7.95}Ni_{17.45}$. The composition dependence of GFA of these five BMGs can be observed from the table 1. As composition changes, value of the thermodynamic parameter $\Delta G$ ($T_g$) changes and hence the GFA shows a variation for different metallic glasses. Basically, $\Delta G$ is the driving force of nucleation. A lower value of $\Delta G$ implies greater GFA. Crystal nucleation requires a large amount of energy. Crystallization of alloy becomes more and more difficult as $\Delta G$ decreases, thereby increasing the GFA of metallic alloys. The value of $\Delta G$ ($T_g$) calculated by equations (5) and (6) are shown in table 1. Zr-based metallic glasses can be arranged in order increasing GFA as $Zr_{65}Al_{8.7}Cu_{14.4}Ni_{11.9}$, $Zr_{64}Al_{10.1}Cu_{11.7}Ni_{14.2}$, $Zr_{63.5}Al_{10.7}Cu_{10.7}Ni_{15.1}$, $Zr_{63}Al_{11.4}Cu_{9.3}Ni_{16.3}$, and $Zr_{62.5}Al_{12.1}Cu_{7.95}Ni_{17.45}$.

## 4. Conclusion

The GFA of Zr-based metallic glasses are studied based on the various GFA parameters. Various GFA parameters were correlated with $Z_{max}$, in order to find their applicability for Zr-based metallic glasses. Statistically, most of them ($\gamma_m$, $\alpha$, $\delta$, $\xi$, $\Phi$, $\omega$, $\omega_2$, $\omega'$, $\beta$, $\beta'$) were found to be a good representative of the GFA of metallic glasses. Thus, the GFA of metallic glasses is composition and characteristic temperature dependent. $\Delta G$ ($T_g$) was found to be the best GFA indicator with statistical correlation factor $R^2$ equal to 0.955 and 0.944 respectively as calculated by Lad-1 (eq.5) and Lad-2 (eq.6) expressions. The amorphous alloys with composition $Zr_{62.5}Al_{12.1}Cu_{7.95}Ni_{17.45}$ was the best glass former among all five metallic glasses, with $\Delta G$ ($T_g$) 5.166 and 4.359 kJmol$^{-1}$ respectively by Lad-1 and Lad-2 expression.

### Acknowledgments

The author, Supriya Kasyap, is grateful to UGC for providing financial assistance under the UGC-RFSMS fellowship scheme. The author, Sonal Prajapati, is grateful to the Department of Science & Technology (DST), Govt. of India, for and DST-INSPIRE fellowship scheme.

### References

1. A. Inoue, T. Zhang and T. Masumoto, *Mater. Trans. Jpn. Inst. Met.*, 31**,** 177 **(1990).**
2. A. Inoue, N. Nishiyama and T. Matsuda, *Mater. Trans. Jpn. Inst. Met.*, 37, 181 **(1996).**
3. A. Inoue, N. Nishiyama and Kimura, *Mater. Trans. Jpn. Inst. Met.*, 38,179 **(1997).**
4. N. Nishiyama and A. Inoue, *Appl. Phys. Lett.*, 80, 568 **(2002).**
5. D. Turnbull, *Contemp. Phys.* 10(5), 473 **(1969).**
6. Z. P. Lu and C. T. Liu, *Acta. Mater.* 50 (13), 3501 **(2002).**
7. Z. Z. Yuan, S. L. Bao, Y. Lu, D. P. Zhang and L. Yao, *J. Alloys Compd.*, 459, 251 **(2008).**
8. Q. J. Chen, J. Shen, D. Zhang, H. B. Fan, J. F. Sun and D. G. McCartney, *Mater. Sci. Eng. A.*, 433, 155 **(2006).**
9. X. H. Du, J. C. Huang, C.T. Liu and Z. P. Lu, *J. Appl. Phys.*, 101,086108 **(2007).**
10. K. Mondal and B. S. Murty, *J. Non-cryst. Solids.* 351, 1366 **(2005).**
11. X. H. Du and J. C. Huang, *Chin. Phys. B.*, 17, 249 **(2008).**

12. Z. L. Long, H. Q. Wei, Y. H. Ding, P. Zhang, G. Q. Xie and A. Inoue, *J. Alloys. Compd.*, 475, 207 **(2009)**
13. P. Zhang, H. Q. Wei, X. L. Wei, Z. L. Long and X. P. Su, *J. Non-Cryst. Solids.*, 355, 2183 **(2009).**
14. G. J. Fan, H. Choo and P. K. Liaw, *J Non-Cryst. Solids.*, 353, 102 **(2007).**
15. S. Guo and C. T. Liu, *Intemetallics*, 18(5), 2065 **(2010).**
16. X. L. Ji and Y. Pan, *Trans. Nonferrous. Met. Soc. China.*, 19(5), 1271 **(2009).**
17. X. Xiao, S. Fang, G. Wang, Q. Hua and Y. Dong, *J. Alloys Compd.*, 376, 145 **(20040.)**
18. J. D. Hoffman, *J. Chem. Phys.*, 29,1192 **(1958).**
19. C. V. Thompson and F. Spaepen, *Acta. Metall.*, 27,1855 **(1979).**
20. L. Battezatti and E. Garonne, *Z. Metallk.*, 75, 305 **(1984).**
21. K. N. Lad, A. Pratap and K. G. Raval, *J. Mater. Sci. Lett.*, 21, 1419 **(2002).**
22. K. N. Lad, K. G. Raval and A. Pratap, *J. Non-Cryst. Solids.*, 334 & 335, 259 **(2004).**
23. X. H. Lin and W. L. Johnson, *J. Appl. Phys.*, 78, 6514 **(1995).**
24. A. H. Cai, X. Xiong, Y. Liu, W. K. An, J. Y. Tan and Y. Pan, *J. Alloys Compds.*, 468, 432 **(2009).**

**Table captions**

Table 1. The melting enthalpy ($\Delta H_m$), Critical dimension ($Z_{max}$), glass transition temperature ($T_g$), crystallization temperature ($T_x$), melting temperature ($T_m$), and Gibbs free energy difference at $T_g$.

Table 1. Kasyap et al

| **Alloy Compositions [24]** | $\Delta H_m$ **[24] (kJmol$^{-1}$)** | $Z_{max}$ **[24] (mm)** | $T_g$ **[24] (K)** | $T_x$ **[24] (K)** | $T_m$ **[24] (K)** | $\Delta G\ (T_g)$ **[Eq (5)] (kJmol$^{-1}$)** | $\Delta G\ (T_g)$ **[Eq (6)] (kJmol$^{-1}$)** |
|---|---|---|---|---|---|---|---|
| $Zr_{62.5}Al_{12.1}Cu_{7.95}Ni_{17.45}$ | 19.39 | 7.5 | 668±1 | 738±1 | 1111±1 | 5.166 | 4.359 |
| $Zr_{63}Al_{11.4}Cu_{9.3}Ni_{16.3}$ | 19.52 | 6.5 | 663±1 | 732±1 | 1103±1 | 5.203 | 4.390 |
| $Zr_{63.5}Al_{10.7}Cu_{10.7}Ni_{15.1}$ | 19.65 | 6 | 653±1 | 724±1 | 1100±1 | 5.252 | 4.432 |
| $Zr_{64}Al_{10.1}Cu_{11.7}Ni_{14.2}$ | 19.76 | 5 | 657±1 | 717±1 | 1098±1 | 5.272 | 4.449 |
| $Zr_{65}Al_{8.7}Cu_{14.4}Ni_{11.9}$ | 20.02 | 4 | 647±1 | 709±1 | 1125±1 | 5.365 | 4.537 |

**Figure captions**

Figure 1. (a) - (f) Relationship between various GFA parameters with $Z_{max}$

Figure 2. (a) Relationship between $\Delta G$ ($T_g$) and $Z_{max}$, (b) Relationship between $\Delta G$ ($T_g$) / $\Delta H_m$ and $Z_{max}$

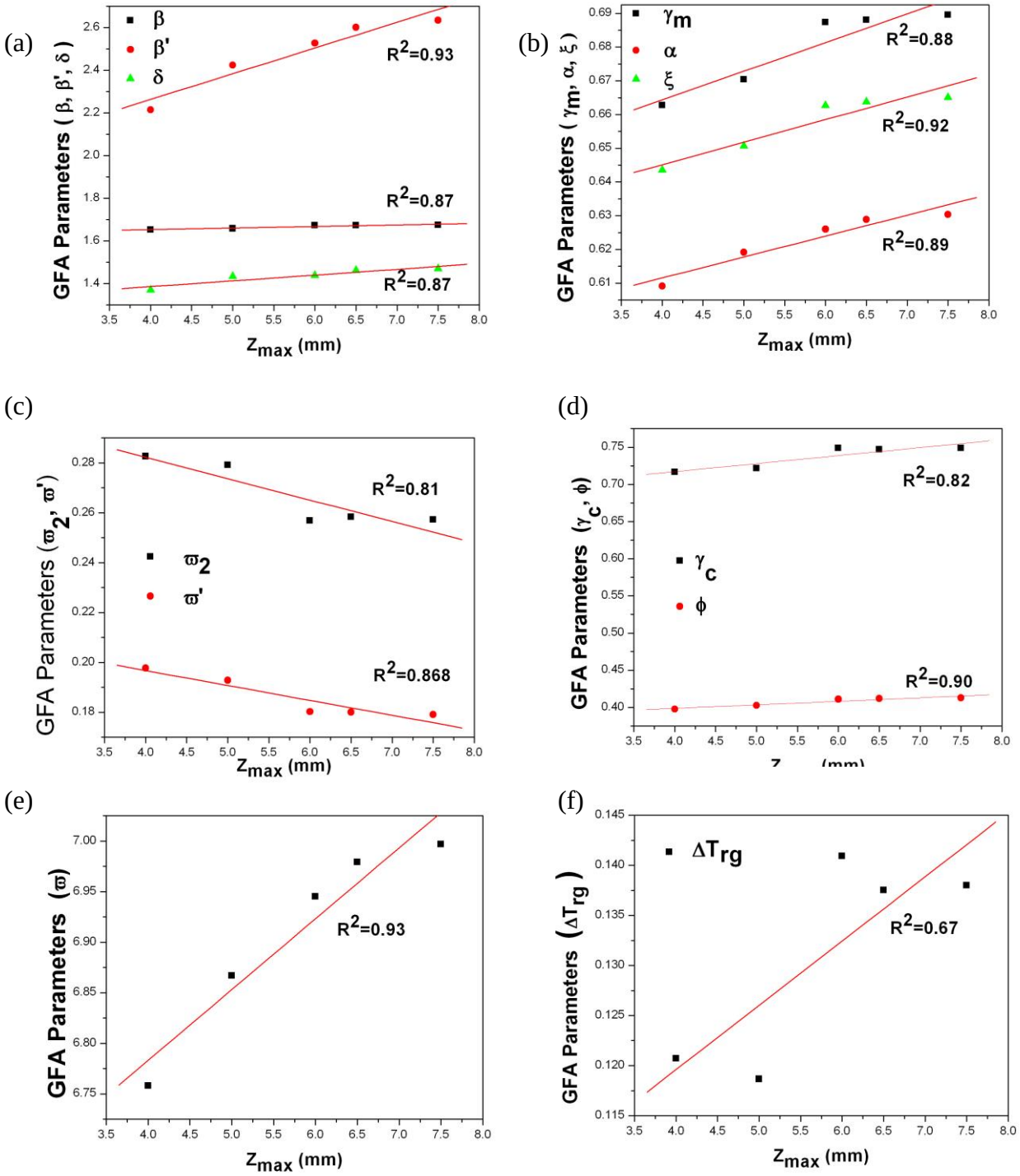


Figure 1. Kasyap et al

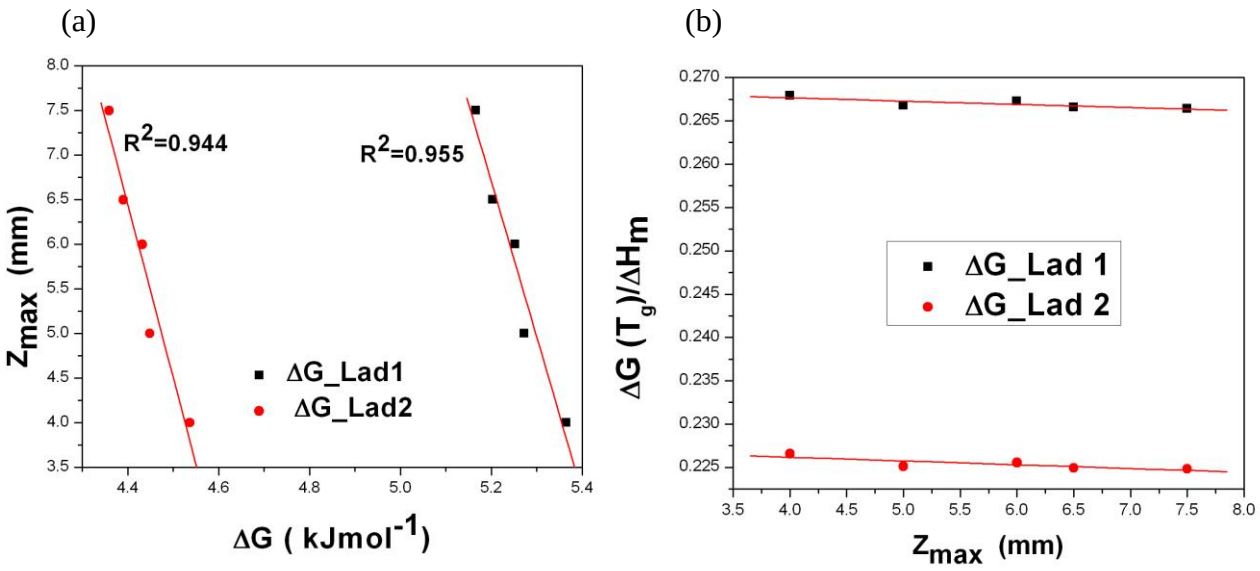


Figure 2. Kasyap et al